Sarcoidosis from Head to Toe: What the Radiologist Needs to Know

Dhakshinamoorthy Ganeshan, MD
Christine O. Menias, MD
Meghan G. Lubner, MD
Perry J. Pickhardt, MD
Kumaresan Sandrasegaran, MD
Sanjeev Bhalla, MD

Abbreviation: ^{18}F FDG = fluorine 18 fluorodeoxyglucose

RadioGraphics 2018; 38:1180–1200

https://doi.org/10.1148/rg.2018170157

Content Codes: CA CH CT GI GU MK NR

From the Department of Radiology, University of Texas MD Anderson Cancer Center, Pickens Academic Tower, 1400 Pressler St, Unit 1473, Houston, TX 77030-4009 (D.G.); Department of Radiology, Mayo Clinic Arizona, Phoenix/Scottsdale, Ariz (C.O.M.); Department of Radiology, University of Wisconsin School of Medicine and Public Health, Madison, Wis (M.G.L., P.J.P.); Department of Radiology, Indiana University School of Medicine, Indianapolis, Ind (K.S.); and Mallinckrodt Institute of Radiology, Section of Abdominal Imaging, Washington University School of Medicine, St Louis, Mo (S.B.). Recipient of a Certificate of Merit award for an education exhibit at the 2016 RSNA Annual Meeting. Received June 6, 2017; revision requested September 7 and received October 2; accepted November 6. For this journal-based SA-CME activity, the authors M.G.L., P.J.P., and K.S. have provided disclosures (see end of article); all other authors, the editor, and the reviewers have disclosed no relevant relationships. **Address correspondence to** D.G. (e-mail: *dganeshan@mdanderson.org*).

SA-CME LEARNING OBJECTIVES

After completing this journal-based SA-CME activity, participants will be able to:

- Describe the histopathologic features and clinical presentation of sarcoidosis.
- Identify characteristic multimodality imaging features of sarcoidosis that affect multiple organ systems, from head to toe.
- Discuss the differential diagnoses for pulmonary and extrapulmonary sarcoidosis.

See www.rsna.org/learning-center-rg.

Sarcoidosis is a multisystem granulomatous disorder characterized by development of noncaseating granulomas in various organs. Although the etiology of this condition is unclear, environmental and genetic factors may be substantial in its pathogenesis. Clinical features are often nonspecific, and imaging is essential to diagnosis. Abnormalities may be seen on chest radiographs in more than 90% of patients with thoracic sarcoidosis. Symmetric hilar and mediastinal adenopathy and pulmonary micronodules in a perilymphatic distribution are characteristic features of sarcoidosis. Irreversible pulmonary fibrosis may be seen in 25% of patients with the disease. Although sarcoidosis commonly involves the lungs, it can affect virtually any organ in the body. Computed tomography (CT), magnetic resonance imaging, and positron emission tomography/CT are useful in the diagnosis of extrapulmonary sarcoidosis, but imaging features may overlap with those of other conditions. Familiarity with the spectrum of multimodality imaging findings of sarcoidosis can help to suggest the diagnosis and guide appropriate management.

Introduction

Sarcoidosis is an idiopathic systemic granulomatous disorder characterized by the development of noncaseating granulomas in various organs (Figs 1–3). It is a global disease with a worldwide incidence of 1–40 cases per 100 000 people per year and a prevalence of 0.2–64 cases per 100 000 people (1–3). Although sarcoidosis is diagnosed in people of all races, there are substantial differences in the incidence depending on race, ethnicity, age, sex, and geography. For example, the incidence is low in Japan compared with that in northern European countries (2). In the United States, it is more common among African Americans (36 cases per 100 000 people) than in white people (11 per 100 000 people) (1); and it is slightly more common in women. Sarcoidosis predominantly develops in patients 25–45 years old, although children and elderly patients may be affected (4–6).

The etiology of sarcoidosis remains unclear. Numerous studies have shown that both environmental and genetic factors may contribute to pathogenesis (4–6). Exposure to insecticides, mold, inorganic particles, and agricultural chemicals has been reported to increase the risk of sarcoidosis (6). Individuals involved in firefighting, metal processing, and the U.S. Navy service have been shown to have a higher risk for developing this disease. The first responders in the World Trade Center terrorist attack of September 11, 2001, were reported to have a high incidence of sarcoidosis (7).

Currently, there is no definite evidence to suggest that sarcoidosis is an infectious or communicable disease. However, the presence of mycobacterial and propionibacterial DNA was reported in tissue samples from patients with sarcoidosis. Indeed, a recent meta-analysis (8) that included 58 studies involving more than 6000 patients

TEACHING POINTS

- Approximately 10%–30% of patients with sarcoidosis have ocular abnormalities, cutaneous lesions, or peripheral lymphadenopathy.
- Well-defined micronodules measuring 2–5 mm with a perilymphatic distribution along the bronchovascular bundles, interlobular septa, interlobar fissures, and subpleural regions are characteristic CT findings seen in pulmonary sarcoidosis.
- Although sarcoidosis typically manifests with symmetric hilar and mediastinal adenopathy, perilymphatic micronodules, and fibrotic changes, it can be associated with a wide range of atypical imaging features. Sarcoidosis may manifest as asymmetric or unilateral hilar or mediastinal adenopathy, which can mimic lymphoma, metastatic adenopathy, tuberculosis, or other granulomatous disorders. Similarly, a spectrum of atypical pulmonary parenchymal abnormalities have been described in sarcoidosis, including mass-like opacities, confluent alveolar opacities (alveolar sarcoid), bulky confluent pulmonary masses, ground-glass opacities, interlobular septal thickening, fibrocystic changes, and miliary opacities.
- Cardiac sarcoidosis can result in various cardiac abnormalities including atrioventricular block, bundle branch block, ventricular tachycardia, heart failure, and sudden death.
- Leptomeningeal sarcoidosis may manifest as diffuse or nodular thickening and enhancement of the leptomeninges on contrast-enhanced T1-weighted MR images.

with sarcoidosis reported that propionibacterium and mycobacteria may be associated with the development of sarcoidosis.

Familial clustering in sarcoidosis has been reported in 4%–17% of cases (5,9). Sverrild et al (10) reported an 80-fold increased risk of developing sarcoidosis in monozygotic twins, which further lends support to genetic susceptibility for sarcoidosis. Human leukocyte antigen type may also be important in sarcoidosis, with certain human leukocyte antigen subtypes resulting in increased risk of its progressive form, while others may be associated with spontaneous resolution (11). The Sarcoidosis Genetic Analysis (SAGA) study reported that molecular cytogenetics may be important to disease susceptibility and clinical presentation in patients with sarcoidosis (12).

In studies (3,13,14), authors hypothesized that sarcoidosis is a cell-mediated immune response to unidentified antigens in genetically susceptible patients. The sarcoid granuloma may develop as part of a multistep process, where the antigens result in activation of macrophages and dendritic cells, which activate CD4 T cells through class II major histocompatibility complex molecules (2,13,14). The characteristic histologic feature of sarcoidosis is the presence of noncaseating granulomas (Fig 3) (14–16). The center of the sarcoid granuloma contains epithelioid cells, macrophages, multinucleated giant cells, and CD4+ T cells, while CD8+ T lymphocytes, B lymphocytes, and fibroblasts are seen at the periphery (13–16). Asteroid bodies, Schaumann bodies, calcium oxalate crystals, and Hamazaki-Wesenberg bodies may develop in the granulomas. The presence of necrosis should lead to a search for an alternative diagnosis because this finding is rare in sarcoidosis, with the exception of a controversial rare sarcoid variant called necrotizing sarcoid granulomatosis (15,16).

In this review, we discuss the clinical and imaging features of pulmonary and extrapulmonary sarcoidosis.

Clinical Features and Diagnostic Workup

The diagnosis of sarcoidosis requires histologic confirmation of noncaseating granulomas from tissue biopsy, presence of clinical-radiologic features, and exclusion of other possible infectious and granulomatous conditions. Often there is a long delay in diagnosis because patients may be clinically asymptomatic despite the presence of abnormalities on chest radiographs (3). Nonspecific respiratory symptoms such as cough, dyspnea, and chest pain may be seen in 9%–19% of cases (3,17). Approximately 10%–30% of patients have ocular abnormalities, cutaneous lesions, or peripheral lymphadenopathy (3,4,6,13,18). Erythema nodosum and acute ankle arthritis may be the presenting symptoms of acute sarcoidosis in 7%–27% of patients (3). Generalized fatigue is a common albeit nonspecific symptom seen in many patients (3).

Patients suspected of having sarcoidosis should undergo comprehensive evaluation that includes obtaining a thorough clinical history and performing a physical examination and chest radiography (3). Serum interleukin-2 receptor, neopterin, angiotensin-converting enzyme, chitotriosidase, lysozyme, plasma *N*-terminal probrain natriuretic peptide, and troponin T levels may be useful biomarkers for disease activity (3). Chest radiography is the most common imaging modality used for pulmonary sarcoidosis, but CT is used frequently for a more comprehensive evaluation. Imaging for extrapulmonary sarcoidosis depends on the site of suspected involvement and often requires CT and magnetic resonance (MR) imaging.

Pulmonary Sarcoidosis

Radiographic abnormalities in the chest are seen in more than 90% of patients with thoracic sarcoidosis (6,17). Symmetric hilar lymphadenopathy is a characteristic imaging finding seen in most patients with thoracic sarcoidosis (Fig 1) (19–21). Mediastinal adenopathy is common, especially that involving the right paratracheal and aortopulmonary window nodal stations. Although other conditions such as lymphoma, tuberculosis, and metastases also may cause hilar and mediastinal adenopathy, sarcoidosis typically results in symmetric involvement, which

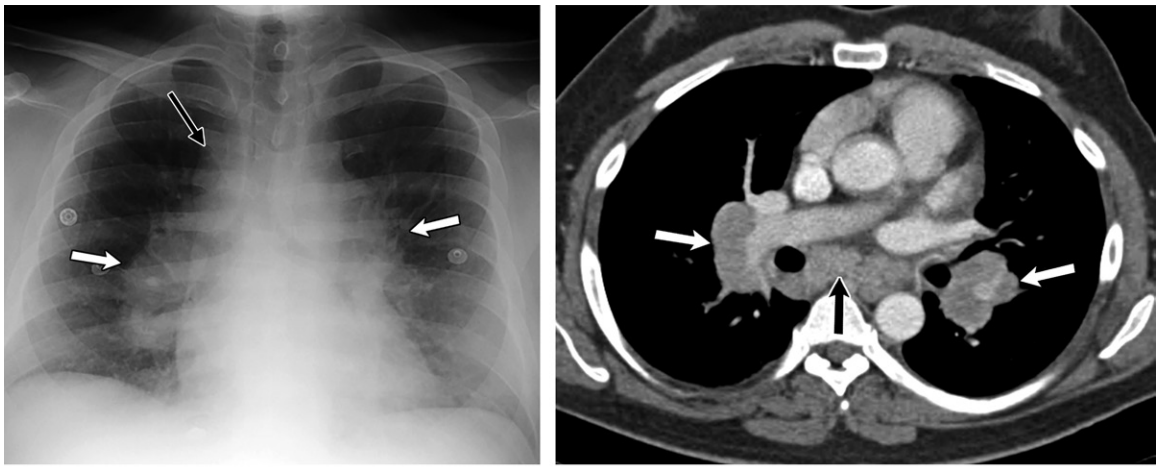

a. b.

Figure 1. Pulmonary sarcoidosis in a 32-year-old woman. Posteroanterior chest radiograph **(a)** and axial chest computed tomographic (CT) image (mediastinal window) **(b)** show bilateral hilar (white arrows) and mediastinal (black arrow) adenopathy.

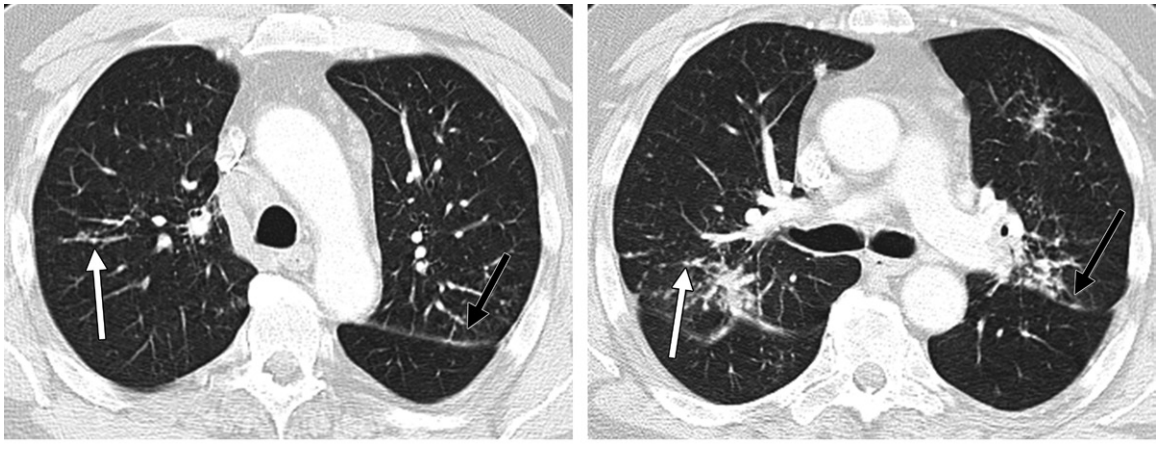

a. b.

Figure 2. Pulmonary sarcoidosis in a 24-year-old man. Axial thin-section chest CT images show pulmonary micronodules in a perilymphatic distribution, including perifissural nodules (black arrow) and peribronchovascular nodules (white arrow).

can help to distinguish it from other entities. Furthermore, lymphadenopathy in sarcoidosis typically does not compress the adjacent vasculature, unlike malignancies that tend to cause a mass effect on surrounding structures.

Chest radiographs may show a range of pulmonary parenchymal abnormalities including micronodules (often with a perilymphatic distribution), macronodules (often with a peribronchovascular distribution), reticulonodular opacities, ground-glass changes, and pulmonary fibrosis (Fig 4). In 1961, Scadding (22) reported on a radiographic staging system for sarcoidosis. Stage 0 (seen in 5%–15% of patients with sarcoidosis) refers to sarcoidosis that is occult on chest radiographs. In stage I sarcoidosis, chest radiographs show only thoracic adenopathy (in 25%–65% of patients with sarcoidosis) (22). In stage II, chest radiographs show thoracic adenopathy and pulmonary infiltrates (in 25%–65% of patients) (22). In stage III sarcoidosis, chest radiographs show only pulmonary infiltrates (in 10%–15% of patients). Stage IV sarcoidosis manifests as pulmonary fibrosis on chest radiographs and accounts for 5% of all cases of sarcoidosis (22). More than 90% of patients with stage I disease identified on chest radiographs may recover completely without treatment (22). In comparison, the recovery rate in untreated patients with stage IV disease essentially decreases to 0% (22).

The presence of characteristic chest radiographic abnormalities in the correct clinical context may be sufficient for diagnosis of sarcoidosis. However, further evaluation frequently is performed with CT, which is more sensitive for detection of parenchymal abnormalities and thoracic lymphadenopathy (Figs 1, 2, 4) (20). CT also may be useful in patients for whom there is a high clinical suspicion for complications such as aspergilloma, concurrent infection, or malignancy. CT can

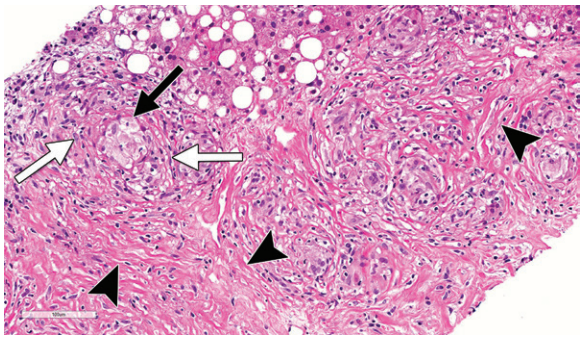

Figure 3. Node biopsy–confirmed sarcoidosis in a 51-year-old woman with thoracic nodes and hepatic involvement. Photomicrograph (hematoxylin-eosin stain; original magnification, ×34) shows a central giant cell (black arrow) within a central collection of epithelioid cells, surrounded by a rim of lymphocytes (white arrows) in the periphery. Collagen bands (arrowheads) also are seen.

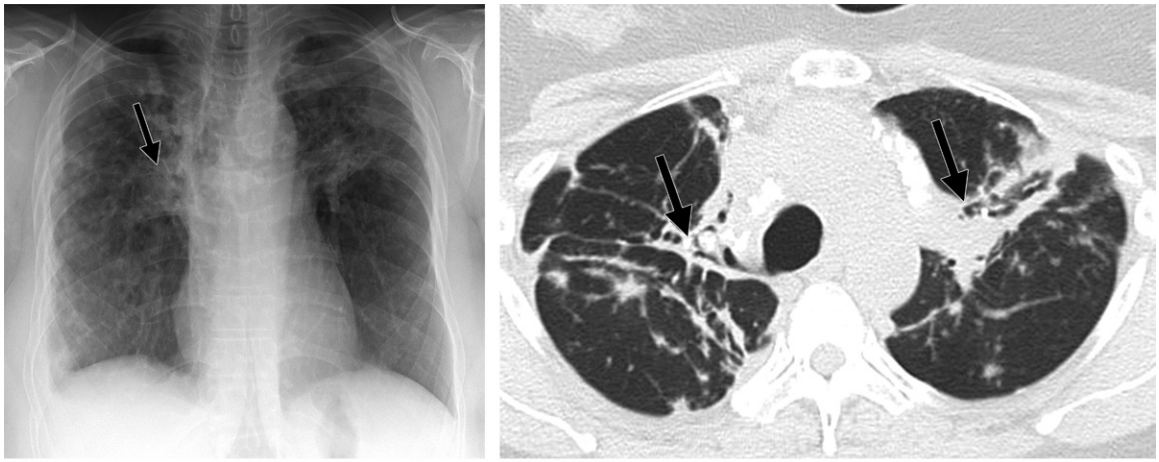

a. **b.**

Figure 4. Pulmonary sarcoidosis in a 48-year-old man. Posteroanterior chest radiograph **(a)** and axial chest CT image **(b)** show central bronchial distortion (arrows), reticulonodular opacities, and volume loss consistent with pulmonary fibrosis.

be helpful for guiding transbronchial biopsy and endobronchial ultrasonographically (US)-guided fine-needle aspiration. Thin-section CT is optimal for assessment of pulmonary parenchymal abnormalities. Well-defined micronodules measuring 2–5 mm with a perilymphatic distribution along the bronchovascular bundles, interlobular septa, interlobar fissures, and subpleural regions are characteristic CT findings seen in pulmonary sarcoidosis (Fig 2) (23). Nodules tend to occur more commonly in the middle to upper lung zones. Air trapping at expiratory CT also is seen frequently in sarcoidosis.

Numerous CT-based scoring systems have been developed for evaluation of the correlation between CT findings and pulmonary function test results in pulmonary sarcoidosis (24,25). A recent CT scoring system based on nodularity, ground-glass opacification, interlobular septal thickening, and consolidation was reported to allow quantification of disease activity and prediction of forced vital capacity response to therapy at 1 year (24). Walsh et al (25) reported that both the visual assessment of the extent of lung fibrosis and the ratio of the diameter of the main pulmonary artery to the diameter of the ascending aorta at nonenhanced CT may provide additional prognostic information. The authors used an integrated clinical-radiologic staging system combining a composite physiologic index (derived from diffusion capacity of carbon monoxide, forced vital capacity, and forced expiratory volume in 1 second) and thin-section CT imaging features (eg, the presence and extent of fibrosis, ground-glass opacification, emphysema, and traction bronchiectasis) and reported that this combined staging algorithm was more predictive of mortality than was any single feature on its own (25).

Although sarcoidosis typically manifests with symmetric hilar and mediastinal adenopathy, perilymphatic micronodules, and fibrotic changes, it can be associated with a wide range of atypical imaging features (21,26–28). Sarcoidosis may manifest as asymmetric or unilateral hilar or mediastinal adenopathy, which can mimic lymphoma, metastatic adenopathy, tuberculosis, or other granulomatous disorders. Similarly, atypical pulmonary parenchymal abnormalities have been described in sarcoidosis, including mass-like opacities, confluent alveolar opacities (alveolar sarcoid), bulky confluent pulmonary masses, ground-glass opacities, interlobular septal thickening, fibrocystic changes, and miliary opacities. Tracheobronchial and pleural involvement

(eg, effusion, chylothorax, hemothorax, pleural thickening, and pleural plaques) also may occur infrequently. Such atypical imaging features can pose a substantial diagnostic challenge.

Differential diagnoses may include a wide spectrum of disorders such as bronchiolitis, lymphangitic carcinomatosis, hypersensitivity pneumonitis, Langerhans cell histiocytosis, usual interstitial pneumonia, cryptogenic organizing pneumonia, and nonspecific interstitial pneumonia. Clinical correlation and histologic evaluation may be required for definitive diagnosis.

Pulmonary fibrosis may develop in 20%–25% of patients with sarcoidosis (Fig 4). Typically, these fibrotic changes are seen along the upper and middle zones of the lungs. Abehsera et al (29) reviewed CT examinations of 80 sarcoidosis patients with pulmonary fibrosis and identified three main CT patterns, each associated with a different functional profile. Forty-seven percent of the patients had predominant central bronchial distortion, which was associated with obstruction and air trapping; 29% had peripheral honeycombing, which was associated with restriction and lower diffusion capacity of the lung for carbon monoxide; and 24% had a diffuse linear pattern, which had minimal functional impairment.

In addition to pulmonary fibrosis, other complications such as pulmonary hypertension and mycetoma may be associated with thoracic sarcoidosis (30). CT is more sensitive for diagnosis of pulmonary arterial hypertension than is radiography and may demonstrate a dilated pulmonary trunk of greater than 29 mm in diameter and enlarged right and left pulmonary arteries (26). The ratio of the main pulmonary artery to the ascending aorta tends to be greater than 1. Recent studies report that this ratio may be predictive of mortality, independent of all other CT patterns (25). Pulmonary aspergillosis and mycetoma may develop in up to 2% of sarcoidosis patients, but the incidence may be higher in those with pulmonary fibrosis, cystic lung disease, preexisting pulmonary cavities, and bronchiectasis (31).

While radiography and CT are the most commonly used imaging modalities for thoracic sarcoidosis, fluorine 18 (^{18}F) fluorodeoxyglucose (FDG) positron emission tomography (PET) and PET/CT have been shown to be increasingly useful in the management of sarcoidosis, including the diagnosis, staging, evaluation of disease activity, and assessment of treatment response (32,33). Studies (34,35) have reported high sensitivity of PET and PET/CT (94%–100%) for thoracic sarcoidosis. PET/CT may be helpful in detecting sites of extrathoracic involvement, especially those that are occult on anatomic images (36–39). Furthermore, ^{18}F FDG PET findings have been reported to correlate with lung function parameters and can help identify disease activity and severity in sarcoidosis (40). PET/CT also has been reported to be useful for evaluating treatment response in patients with pulmonary and extrapulmonary sarcoidosis (32,33,41–43).

Cardiac Sarcoidosis

Autopsy studies report cardiac involvement in 25% of sarcoidosis cases, but clinically evident disease is seen in only 5% of cases (2,44). Cardiac involvement in sarcoidosis may be associated with high mortality and accounts for 13%–25% of sarcoidosis-related deaths in the United States. The mortality rates are higher in Japan, where cardiac involvement accounts for up to 85% of sarcoidosis-related deaths (44). Patients may be clinically asymptomatic; studies (45–47) report that 13%–39% of patients with sarcoidosis may have clinically silent cardiac sarcoidosis, despite imaging studies showing cardiac involvement. When symptomatic, patients may present with chest pain, palpitations, dyspnea, and syncope. Cardiac sarcoidosis can result in various cardiac abnormalities including atrioventricular block, bundle branch block, ventricular tachycardia, heart failure, and sudden death (48,49).

Approximately 16%–35% of patients younger than 60 years who present with an unexplained complete atrioventricular block or ventricular tachycardia may have cardiac sarcoidosis as the underlying cause (50). In patients with symptomatic cardiac sarcoidosis, the cardiac symptoms dominate the clinical presentation, with only mild extracardiac clinical features. Furthermore, up to one-third of patients with clinically symptomatic sarcoidosis may have isolated cardiac involvement (45,50). Therefore, cardiac sarcoidosis should be considered in the differential diagnosis of any patient, especially younger individuals, who presents with cardiac conduction abnormalities, ventricular arrhythmia, or heart failure of unknown etiology (45,48).

The electrocardiogram may reveal nonspecific abnormalities including an atrioventricular block or a bundle branch block (46,47). Echocardiography may show left ventricular regional wall motion abnormalities, thinning of the basal interventricular septum, thinning of the left ventricular free wall, dilatation of the left ventricle, reduced ejection fraction, and ventricular aneurysms, but none of these findings are specific for cardiac sarcoidosis (47).

The criterion standard for diagnosis of cardiac sarcoidosis is histologic confirmation of noncaseating granulomas by means of endomyocardial biopsy; however, this is an invasive procedure and may be associated with a low diagnostic yield of 20%–50% owing to sampling errors (44,45).

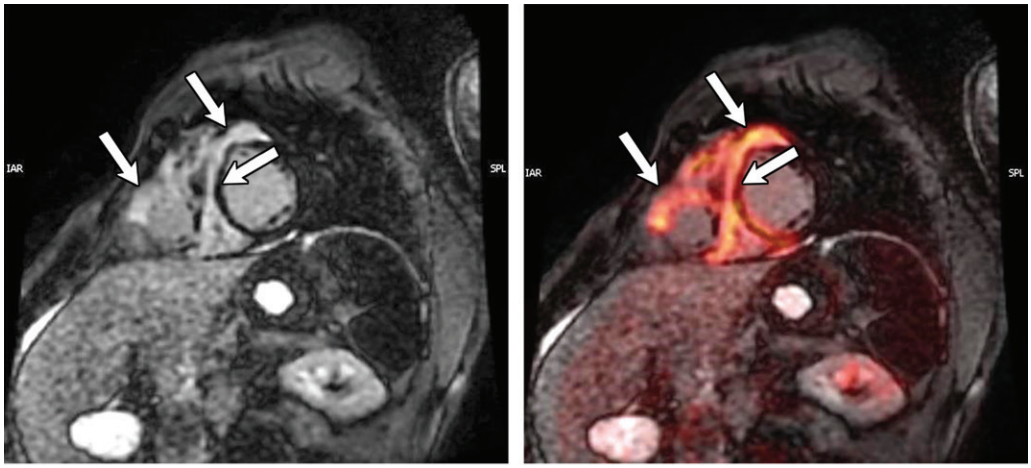

a. b.

Figure 5. Cardiac sarcoidosis in a 45-year-old man with progressively worsening dyspnea on exertion, a new right bundle branch block on an electrocardiogram (not shown), and a 2:1 atrioventricular block during exercise. **(a)** Sagittal cardiac MR image shows patchy areas of delayed gadolinium enhancement (arrows). Localized asymmetric basal septal thinning and right ventricular hypertrophy were also seen. **(b)** Sagittal fused PET/MR image shows heterogeneous FDG uptake (arrows) in the corresponding areas of abnormality.

Imaging, especially cardiac MR imaging and cardiac FDG PET, has an important role in the noninvasive diagnosis of cardiac sarcoidosis and is included in the diagnostic criteria by both the International Heart Rhythm Society Expert Consensus Recommendations on Criteria for Diagnosis of Cardiac Sarcoidosis and the Japanese Ministry of Health and Welfare Guidelines (Fig 5) (51,52). There is no specific pattern of late gadolinium enhancement at cardiac MR imaging that is diagnostic for cardiac sarcoidosis. However, cardiac sarcoidosis usually is associated with patchy and multifocal late gadolinium enhancement in the basal segments, particularly of the septum and the lateral wall, and tends to affect the midmyocardium and epicardium, sparing the subendocardium (53,54).

Cardiac MR imaging can allow identification of clinically silent cardiac sarcoidosis, which may be vitally important and provide an opportunity to better manage the disease and improve prognosis (46,47). There are many conditions to consider in the differential diagnosis of delayed myocardial enhancement on cardiac MR images, including myocardial infarction, myocarditis, and cardiac amyloidosis (54,55). In myocardial infarction, the late gadolinium enhancement typically is limited to the subendocardial or transmural region and characteristically is restricted to the affected vascular territory (54,55).

In myocarditis, cardiac MR imaging may show delayed enhancement in a nonvascular distribution and often is associated with wall abnormalities. Subepicardial enhancement is the dominant pattern in most cases of myocarditis, although transmural enhancement may develop in cases of severe myocardial damage (54,55). The degree of enhancement is reported to become less intense over weeks, especially with scar development. In cardiac amyloidosis, MR imaging often shows biventricular hypertrophy and diffuse or heterogeneous left ventricular wall enhancement (54,55). Correlating the clinical findings with imaging features may be useful in narrowing the differential diagnosis.

^{18}F FDG PET also has an increasingly important role in the diagnosis, management, and prognostication of cardiac sarcoidosis (56). Active sarcoidosis is associated with patchy focal ^{18}F FDG uptake (Fig 5). Comprehensive assessment for cardiac sarcoidosis can be achieved by performing a resting myocardial perfusion sequence with ^{18}F FDG PET (57). A normal result is defined as normal perfusion and normal ^{18}F FDG uptake. On the other hand, the presence of focal ^{18}F FDG uptake with or without a perfusion defect suggests active inflammatory sarcoidosis.

The presence of a perfusion defect without FDG uptake is in keeping with cardiac sarcoidosis associated with myocardial fibrosis and scarring (58). Blankstein et al (57) reported a four-fold increase in the annual rate of ventricular tachycardia or death in the group with both abnormal perfusion defects and abnormal FDG uptake compared with those with normal study results.

Youssef et al (59) reported 89% sensitivity (95% confidence interval: 79%, 96%) and 78% specificity (95% confidence interval: 68%, 86%) for ^{18}F FDG PET in the diagnosis of cardiac sarcoidosis. A more recent meta-analysis (60) that included 16 studies with a total of 559 patients confirmed the high diagnostic accuracy

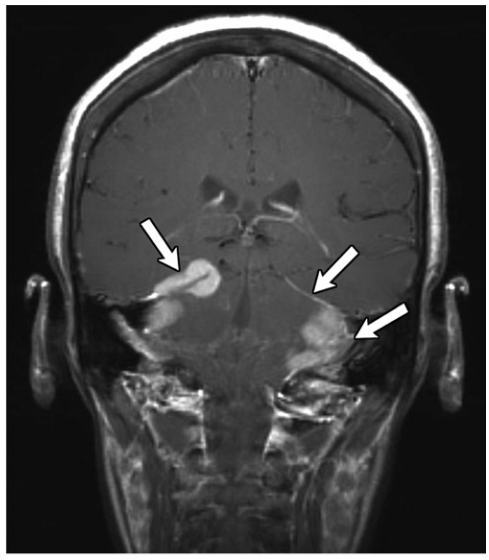

a.

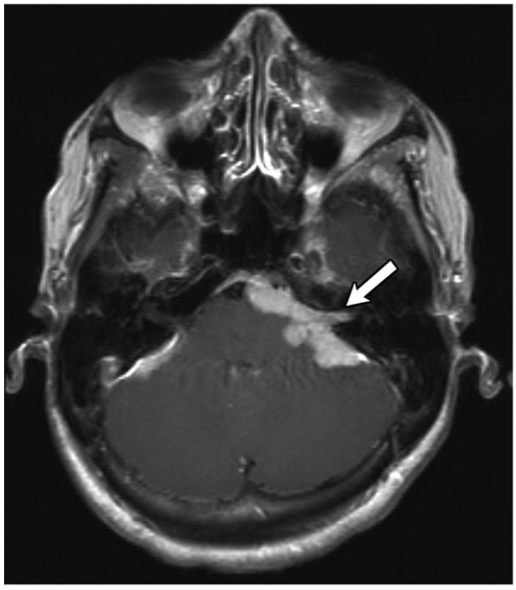

b.

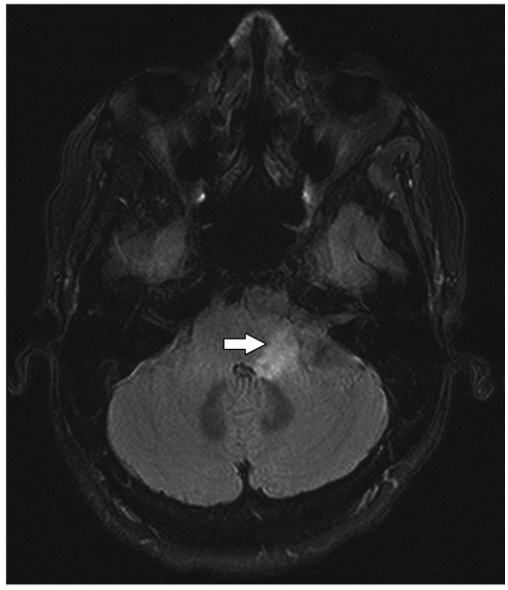

c.

Figure 6. Neurosarcoidosis in a 53-year-old woman. **(a)** Coronal contrast material–enhanced T1-weighted MR image shows thick nodular pachymeningeal enhancement (arrows) along the basilar dura, including near the cerebellopontine angles and tentorial reflections bilaterally. **(b)** Axial contrast-enhanced T1-weighted MR image shows nodular enhancement along the seventh and eighth cranial nerve complex (arrow). **(c)** Axial T2-weighted fluid-attenuated inversion-recovery MR image shows a hyperintense lesion in the left medulla (arrow), a finding consistent with intraparenchymal involvement.

of ^{18}F FDG PET for cardiac sarcoidosis and also reported that this diagnostic accuracy may be substantially affected by the patient's duration of fasting, use of a low-carbohydrate diet, and administration of heparin (for cardiomyocyte glucose uptake suppression) before imaging.

Given the complimentary roles of PET and MR imaging, a combination of the two modalities may add value in diagnosis of cardiac sarcoidosis, especially because cardiac MR imaging is more sensitive for myocardial scarring, whereas PET may be helpful for identification of the early inflammatory stage without any scarring (61).

^{18}F FDG PET also may be useful for monitoring disease activity and evaluating treatment response in patients with cardiac sarcoidosis (62–67). In a study involving 23 patients with cardiac sarcoidosis, a reduction in the intensity and extent of myocardial inflammation at FDG PET after therapy was shown to be significantly associated with improvement in left ventricular ejection fraction (63). The vital role of ^{18}F FDG PET in cardiac sarcoidosis has been acknowledged by the Society of Nuclear Medicine and Molecular Imaging (SNMMI) and the American Society of Nuclear Cardiology (ASNC), which recently released guidelines supporting the use of ^{18}F FDG PET in detection of cardiac sarcoidosis and assessment of treatment response (62).

Neurosarcoidosis

Autopsy studies report a high incidence of subclinical asymptomatic neurosarcoidosis of 25%–50% (68). Clinically recognized symptomatic central nervous system sarcoidosis is present in 5%–15% of all patients with sarcoidosis (Figs 6–8), and most

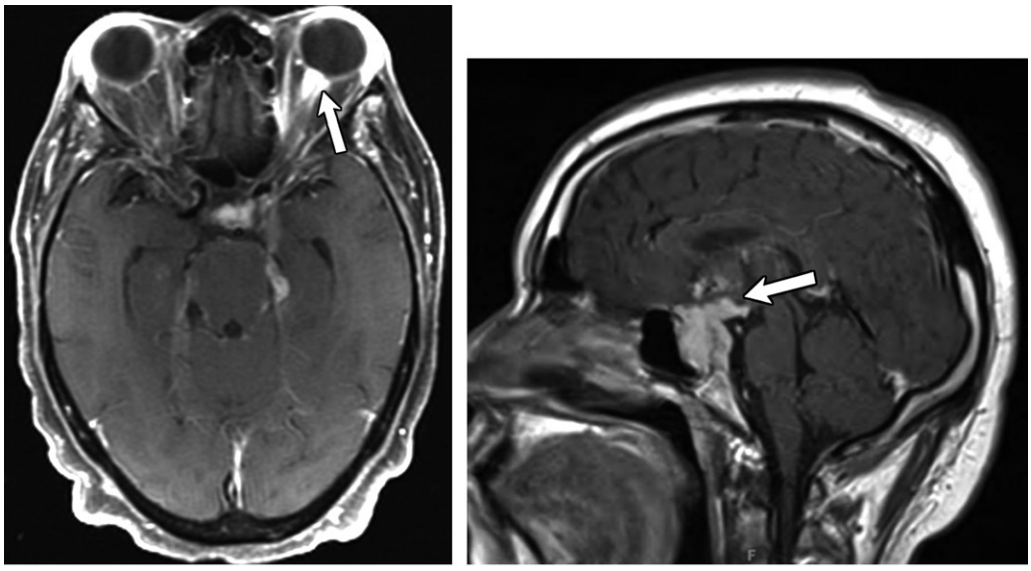

7. 8.

Figures 7, 8. **(7)** Neurosarcoidosis in a 67-year-old woman. Axial contrast-enhanced T1-weighted MR image shows nodular enhancement in the left optic nerve (arrow), sella turcica, and leptomeningeal region. **(8)** Pituitary sarcoidosis in a 32-year-old woman. Sagittal contrast-enhanced T1-weighted MR image shows an avidly and heterogeneously enhancing nodular mass in the sella turcica, extending to the optic chiasm (arrow).

of these patients have extraneural manifestations (6). Isolated central nervous system sarcoidosis is rare, affecting 1% of all patients with sarcoidosis (68). The clinical features of neurosarcoidosis depend on the site of involvement and include facial nerve palsy, vision loss, diplopia, headache, seizure, meningism, weakness, and paresthesia (69).

Cranial nerve involvement, and in particular, facial nerve involvement, is a common manifestation in patients with clinically symptomatic central nervous system sarcoidosis (Fig 6). Bilateral facial nerve palsy may develop in up to one-third of patients with neurosarcoidosis. Patients also may present with Heerfordt syndrome, which includes symptoms such as facial nerve palsy, fever, parotid gland enlargement, and uveitis (3,6,13). Sarcoidosis also may affect other cranial nerves including the olfactory, auditory, and optic nerves (Fig 7). Cranial neuropathy may manifest at MR imaging as abnormal enlargement and enhancement of the involved cranial nerves.

Leptomeningeal involvement in sarcoidosis (sarcoid meningitis) is reported to develop in up to one-third of patients with central nervous system sarcoidosis and may result in hydrocephalus, seizures, or cognitive decline (69). Leptomeningeal sarcoidosis may manifest as diffuse or nodular thickening and enhancement of the leptomeninges on contrast-enhanced T1-weighted MR images (Fig 6) (70).

There may be disruption of the blood-brain barrier, which may result in spread of disease along the cortical sulci, perivascular spaces, and the cisterns around the base of the brain. Multiple small granulomas may coalesce, resulting in intra-axial masses with surrounding edema (71). However, these findings are not specific and may be seen in other conditions such as tuberculosis, lymphoma, and metastases. Correlation with abnormalities of the cerebrospinal fluid may be helpful. In particular, patients who show diffuse leptomeningeal gadolinium enhancement at MR imaging are more likely to harbor cerebrospinal fluid abnormalities (70,71). Dural involvement also is known to occur in sarcoidosis, and focal dural masses tend to be T2 hypointense at MR imaging of the brain (70,71).

Sarcoid granulomas may involve any portion of the brain parenchyma but are found more often in the hypothalamus and pituitary gland, which can result in diabetes insipidus. Imaging findings include plaque-like or nodular thickening in the infundibular stalk and optic chiasm. Lesions may be T1 isointense or T2 hypointense and may show marked enhancement on MR images (Fig 8) (72). Hydrocephalus may be seen in 5%–12% of patients (69). Sarcoidosis that involves the cerebral white matter, cerebellum, and brainstem manifests as multiple tiny T2-hyperintense and T1-hypointense periventricular white matter lesions (69). Active sarcoidosis lesions commonly show enhancement with intravenous gadolinium administration. After therapy, these lesions may show diminished T2 hyperintensity and decreased enhancement (69,73).

Dumas et al (73) classified central nervous system sarcoidosis into three types. Parenchymal lesions that show enhancement on gadolinium-enhanced T1-weighted images are classified as type

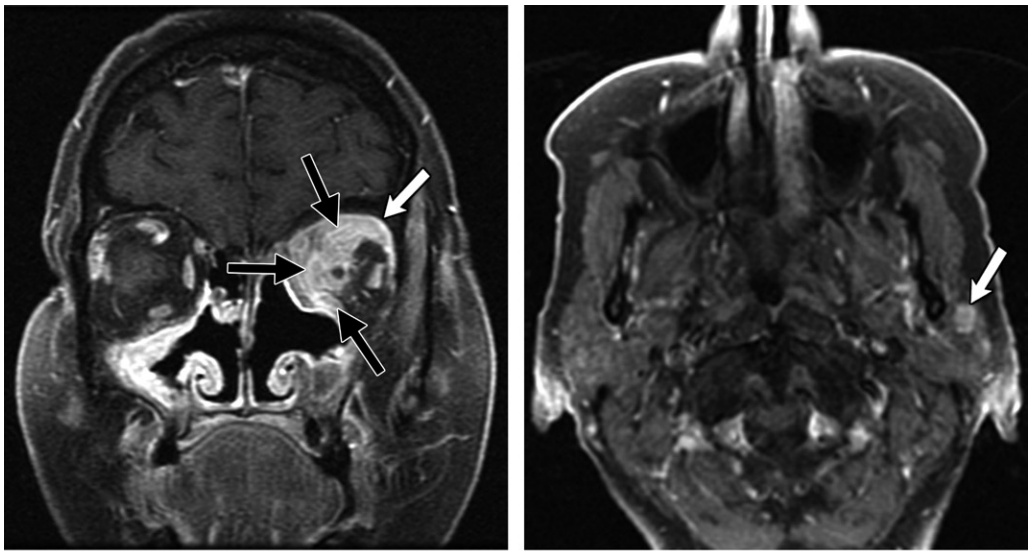

9. 10.

Figures 9, 10. **(9)** Head and neck sarcoidosis in a 32-year-old woman. Coronal contrast-enhanced T1-weighted MR image shows nodular thickening and enhancement of the left lacrimal gland (white arrow) and superior, medial, and inferior recti muscles (black arrows). Nodular thickening and enhancement also are seen in the right lateral rectus muscle and the right maxillary sinus. The differential diagnosis includes consideration of pseudotumor, sarcoidosis, and granulomatosis with polyangiitis. A diagnosis of noncaseating granuloma was confirmed on the basis of biopsy results. **(10)** Head and neck sarcoidosis in a 37-year-old man. Axial contrast-enhanced T1-weighted MR image shows a focal enhancing mass in the left parotid gland. The presence of a noncaseating granuloma was confirmed on the basis of biopsy results and was consistent with a diagnosis of sarcoidosis.

1, while nonenhancing lesions are classified as type 2 (nodular or confluent abnormalities with T2 high signal intensity in the periventricular regions and in the deep white matter, which mimic demyelinating lesions seen in multiple sclerosis) or type 3 (2–8-mm multifocal patchy T2-hyperintense lesions in the subcortical white matter, which mimic those seen in small-vessel atherosclerotic disease). Dumas et al (73) reported that gadolinium enhancement may be a marker for biologically active lesions and that enhancing lesions potentially are reversible and may regress after corticosteroid therapy. In comparison, type 2 and type 3 lesions are irreversible.

Spinal cord involvement tends to manifest in elderly patients, with lesions more commonly seen in the cervicothoracic spine. The clinical features may mimic those seen in cervical spondylitis. Spinal neurosarcoidosis may show a wide spectrum of findings at MR imaging, including leptomeningeal enhancement, fusiform spinal cord enlargement, focal or diffuse intramedullary disease, intradural extramedullary lesions, extradural lesions, and spinal cord atrophy. Typically, the lesions are T1 hypointense and T2 hyperintense and show patchy enhancement (72). Cerebrovascular involvement also has been reported in sarcoidosis and may result in transient ischemic attacks, strokes, and, rarely, even intracranial hemorrhage.

The role of PET/CT in neurosarcoidosis is not yet clear. Authors of case reports and small case series (74–76) suggest that PET/CT may be useful, but larger studies are required before this use becomes the standard of care.

The definitive diagnosis of neurosarcoidosis requires biopsy confirmation (69). However, in most instances, this is not feasible, and a diagnosis of probable neurosarcoidosis can be made on the basis of the clinical evidence such as cerebrospinal fluid abnormalities (eg, elevated cerebrospinal fluid cell counts, elevated protein levels, and the presence of oligoclonal bands), MR imaging features of neurosarcoidosis, confirmation of systemic sarcoidosis (from biopsy of a nonneurologic site, positive results on a Kveim test, or elevated serum angiotensin-converting enzyme plus imaging findings of sarcoidosis at chest imaging or gallium imaging) (69).

Head and Neck Sarcoidosis

Ten percent to 15% of patients with sarcoidosis have head and neck manifestations (77). Any site in the head and neck may be involved, including the orbits, sinonasal regions, pharynx, hypopharynx, salivary glands, thyroid gland, cervical nodes, and larynx (Figs 9–11) (78).

Orbital involvement may be seen in 11%–83% of patients with head and neck sarcoidosis (17,78,79). The uvea, optic nerve, lacrimal gland, extraocular muscles, orbital fat, and soft tissue may be affected (Fig 9). Ocular involvement is fairly common in the orbits and has been reported in 19%–21% of patients with sarcoidosis

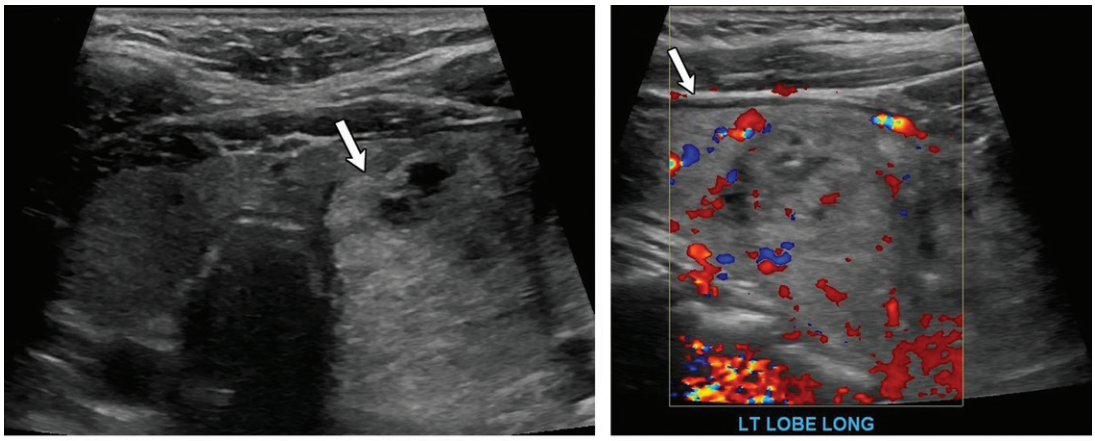

a. b.

Figure 11. Sarcoidosis involving the thyroid gland in a 34-year-old woman. **(a)** US image of the thyroid shows a large heterogeneous nodule in the left thyroid lobe (arrow). **(b)** Color Doppler US image shows mild Doppler flow in the left thyroid nodule. A diagnosis of sarcoidosis was confirmed on the basis of biopsy results. The patient also had a pulmonary sarcoid (not shown).

(80). Anterior uveitis is the most common ocular manifestation (65%–71%), followed by posterior and intermediate uveitis (2). Patients may present with pain, redness, photophobia, blurred vision, and floaters. The diagnosis usually is made on the basis of clinical examination. Optic nerve involvement may result in pain and affect central visual acuity and color vision. Abnormal high signal intensity may be seen in the optic nerve on T2-weighted images, while contrast-enhanced T1-weighted images may reveal nodular thickening and enhancement. However, these appearances are not specific and may be seen in other inflammatory and neoplastic conditions including optic neuritis, lymphoma, and carcinomatosis (81).

The lacrimal gland may be involved in up to 10% of patients with head and neck sarcoidosis, resulting in swollen eyelids or xeropthalmia (81). Both CT and MR imaging may show abnormally enlarged and enhancing lacrimal glands (81). Involvement of the extraocular muscle and orbital fat are rare manifestations of sarcoidosis. CT and MR imaging may show abnormal thickening and enhancement in extraocular muscles and tendons. Heterogeneous, infiltrative, enhancing soft-tissue masses may be seen in the retrobulbar fat.

Parotid gland involvement may occur in 5% of patients with sarcoidosis (Fig 10). The clinical manifestations include enlargement of the parotid gland, xerostomia, and facial nerve palsy. Parotid gland involvement also may occur as part of Heerfordt syndrome. Gallium 67(^{67}Ga)-citrate scintigraphy may show abnormal bilateral uptake in the parotid and lacrimal glands in patients with sarcoidosis, along with normal uptake in the nasopharyngeal mucosa, commonly referred to as "the panda sign" (81). However, this sign is not pathognomonic for sarcoidosis, because lymphoma and Sjögren syndrome also may cause a similar appearance (81).

Sinonasal sarcoidosis may manifest with nonspecific symptoms such as nasal obstruction and rhinosinusitis, which may result in delayed diagnosis (77,78). CT and MR imaging may show nodular thickening and enhancement in the nasal septum and turbinates. Paranasal sinus involvement may result in soft-tissue opacification. More aggressive lesions may be associated with destruction of the adjacent bones and may extend to intracranial structures. Sarcoidosis also can involve the external ear, middle ear, and temporal bone (77).

Rarely, laryngeal structures including the epiglottis, arytenoids, aryepiglottic folds, and false vocal folds may be affected. Mild laryngeal involvement may be clinically silent but can result in hoarseness and dyspnea. In severe cases, patients may present with stridor, mandating urgent tracheostomy. The imaging findings are nonspecific, but the affected regions may show edema and nodular thickening (81).

Sarcoidosis of the thyroid gland has been reported in up to 4% of patients with sarcoidosis in autopsy studies (77,78). US may show diffuse enlargement and nonspecific thyroid nodules (Fig 11). Biopsy may be required to differentiate it from other conditions such as multinodular goiter and malignancies. Cervical adenopathy can occur in up to 40% of patients with head and neck sarcoidosis (6,77,78). CT or MR imaging may reveal homogenously enhancing nodes. Sarcoidosis also may involve the vessels in the head and neck, as in vasculitis involving the carotid arteries. MR imaging may show abnormal soft-tissue thickening encasing the carotid vessels (81).

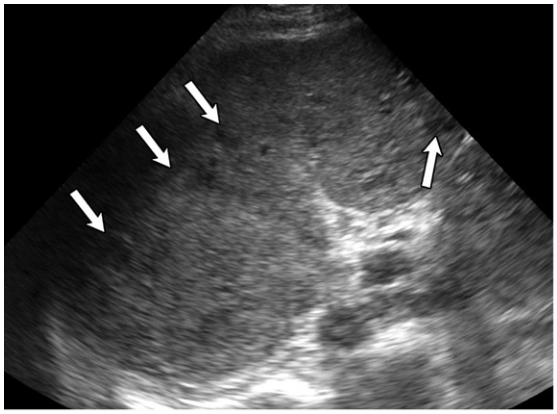

12.

13.

Figures 12, 13. **(12)** Hepatic sarcoidosis in a 50-year-old man. US image shows numerous small poorly defined hypoechoic lesions (arrows). A diagnosis of hepatic sarcoidosis was confirmed on the basis of biopsy results. Small hepatic sarcoid lesions may be difficult to evaluate with US but are often better visualized with CT and MR imaging. **(13)** Hepatosplenic sarcoidosis in a 33-year-old man. Axial CT image of the abdomen shows many tiny hypointense nodules in the liver (white arrows), slightly larger hypointense nodules in the spleen (arrowhead), and multiple upper abdominal nodes (black arrow).

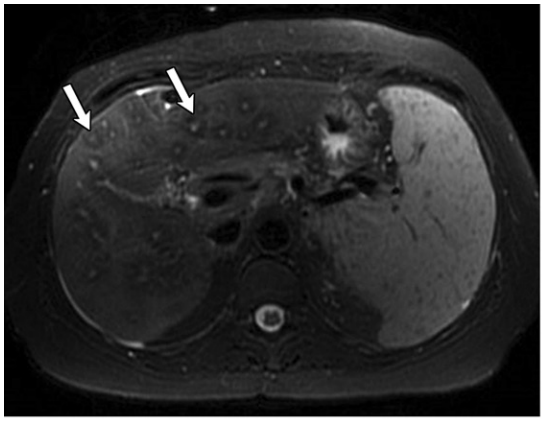

a.

b.

Figure 14. Hepatic sarcoidosis in a 51-year-old woman. **(a)** Axial T2-weighted MR image shows the T2 "halo sign," with hypointense periportal zones (arrows). **(b)** Axial contrast-enhanced portal venous phase MR image shows poor enhancement in the periportal regions (arrows). The presence of hepatic sarcoidosis with prominent tracts of fibrosis along the periportal region was confirmed on the basis of the biopsy results.

Abdominal and Pelvic Sarcoidosis

Sarcoidosis can affect any abdominal organ, but the liver, spleen, peritoneum, kidneys, and stomach are more commonly affected (Figs 12–20) (49). Autopsy studies show that the liver may be involved in 24%–80% of patients with systemic sarcoidosis (23,68). In most cases, hepatic manifestations of sarcoidosis coexist with pulmonary sarcoidosis, but isolated hepatic disease without thoracic involvement may develop in up to 13% of patients (82). Hepatic sarcoidosis is often asymptomatic (23,68). However, symptomatic hepatic involvement that manifests as fatigue, fever, arthralgia, nonspecific abdominal pain, jaundice, and pruritus may occur in 5%–15% of patients. Portal hypertension and cirrhosis can develop in patients with long-standing hepatic sarcoidosis.

US, CT, and MR imaging are commonly used in the evaluation of hepatic sarcoidosis (83). US may show hepatomegaly, heterogeneous liver parenchyma, and increased liver echogenicity (84). US also may reveal innumerable small hypoechoic lesions in 5%–19% of patients (Fig 12a) (85–87). CT is reported to be more sensitive than US for identifying these heterogeneous hypointense nodules, which typically measure only a few millimeters, but larger lesions may develop, especially when the smaller lesions coalesce (Fig 13) (85–87). These sarcoidosis nodules are usually hypointense on both T1- and T2-weighted MR images (88). The differential diagnosis includes evaluation for metastases, lymphoma, fungal microabscesses, and mycobacterial infections. When there is doubt regarding the definitive diagnosis, biopsy may be warranted.

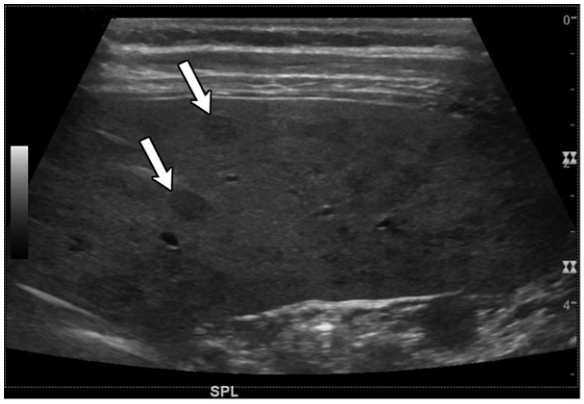

a.

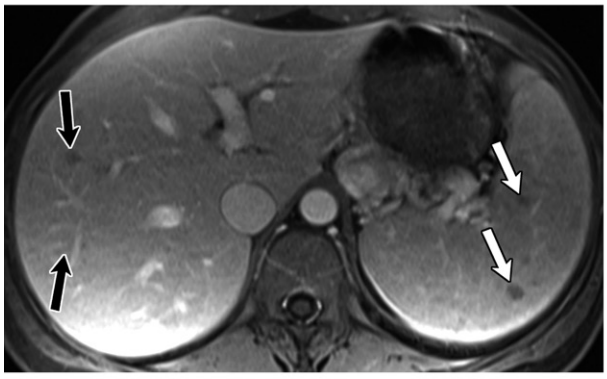

b.

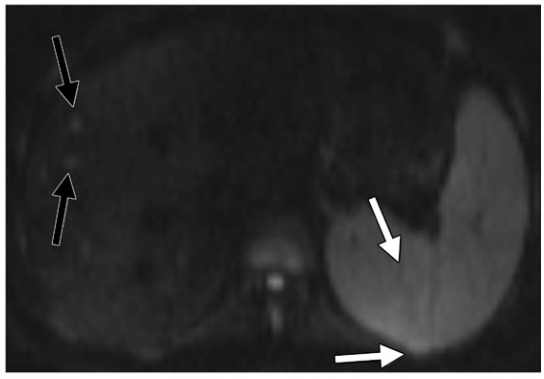

c.

Figure 15. Splenic sarcoidosis in a 38-year-old woman. **(a)** US image shows many small hypointense lesions in the spleen (arrows). **(b)** Axial contrast-enhanced T1-weighted MR image shows small hypovascular lesions in the spleen (white arrows) and liver (black arrows). **(c)** Axial diffusion-weighted image with a high *b* value (800 sec/mm^2) shows many tiny lesions in the spleen (white arrows) and liver (black arrows) with restricted diffusion.

Sarcoidosis granulomas may grow along the portal tracts, which can be seen as areas of increased signal intensity on T2-weighted MR images (84). The T2 "halo sign" often reported with biliary cirrhosis or autoimmune hepatitis also can be seen in patients with hepatic sarcoidosis, manifesting as periportal T2-hypointense zones surrounding the portal triads that also may show decreased enhancement after administration of contrast material (Fig 14). Patients with advanced cases of hepatic sarcoidosis may develop bridging fibrosis and, ultimately, cirrhosis and can present with imaging features of cirrhosis and portal hypertension. Sarcoidosis also can involve the intrahepatic and extrahepatic bile ducts, resulting in biliary dilatation and bile duct strictures (88).

Splenic involvement has been reported in 38%–77% of cases in autopsy studies (19). Splenomegaly is relatively common, occurring in 25%–60% of patients (83,85–87); and granulomas may be seen in the spleen in 6%–33% of patients (83,85–87). The imaging appearance of splenic sarcoidosis nodules mimics that of hepatic sarcoidosis in that the nodules are usually hypoechoic on US images, appear hypointense on CT images, and tend to be hypointense on T1- and T2-weighted MR images (Figs 15–17). In general, focal splenic lesions tend to be larger than hepatic foci. Although sarcoid nodules may show enhancement on delayed phase images, the lack of peripheral discontinuous nodular enhancement in the early phases may help to differentiate them from other entities such as hemangiomas.

Pancreatic involvement is rare and usually is secondary to invasion from adjacent peripancreatic adenopathy, rather than isolated primary pancreatic involvement (49). The imaging features are nonspecific and often indistinguishable from pancreatitis or pancreatic carcinoma, necessitating biopsy for definitive diagnosis.

Although any part of the gastrointestinal luminal tract may be affected in patients with sarcoidosis, the stomach is the most common site of involvement (Fig 17) (83). Barium studies may show nodular gastric mucosa with irregularly thickened folds, aphthous ulcers, and polypoid filling defects. Occasionally, a linitis plastica appearance may be seen with diffuse rigidity of the gastric wall and a narrowed lumen. Involvement of sarcoidosis in the small bowel and colon may result in coarse granular filing defects, mass-like lesions, or circumferential narrowing of the bowel lumen.

Autopsy studies report renal involvement in 7%–22% of patients with sarcoidosis (79). Renal sarcoidosis typically causes interstitial nephritis with an infiltrative pattern that tends to preserve the overall reniform shape of the

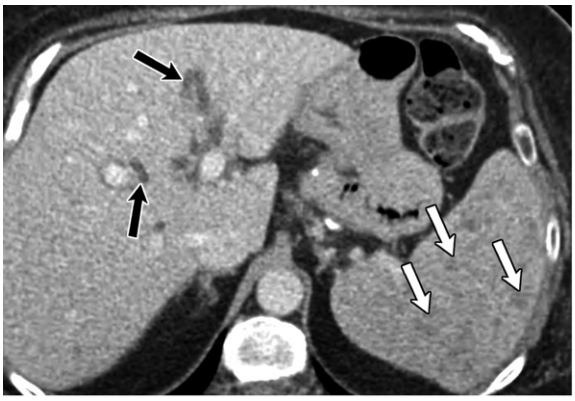

16.

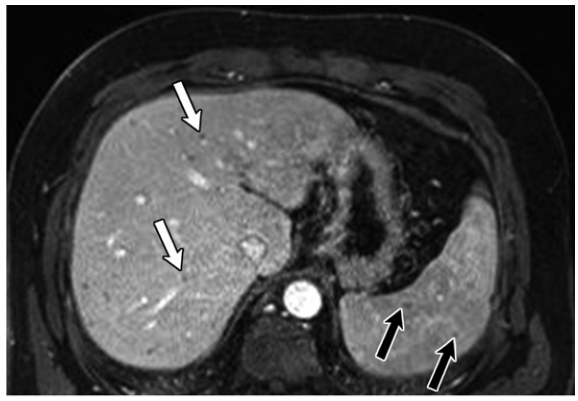

17.

Figures 16, 17. **(16)** Splenic sarcoidosis in a 59-year-old woman. Axial postcontrast CT image shows numerous small hypointense lesions in the spleen (white arrows). Mild biliary dilatation also is seen (black arrows). **(17)** Sarcoidosis involving the esophagus, stomach, liver, and spleen in a 41-year-old man. Axial contrast-enhanced T1-weighted MR image shows tiny hypovascular lesions in the liver (white arrows) and spleen (black arrows). Abnormal heterogeneous thickening and enhancement is also seen in the stomach. A diagnosis of sarcoidosis was confirmed on the basis of biopsy results.

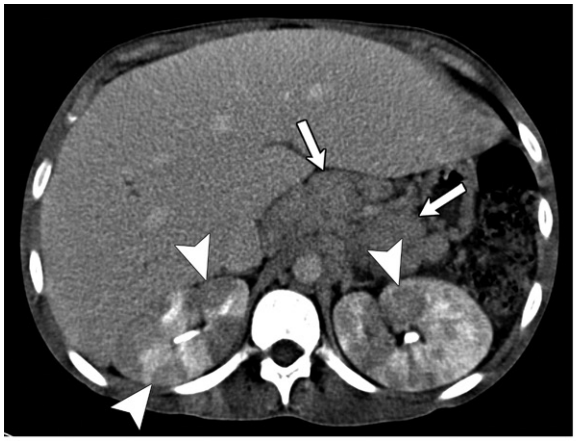

18.

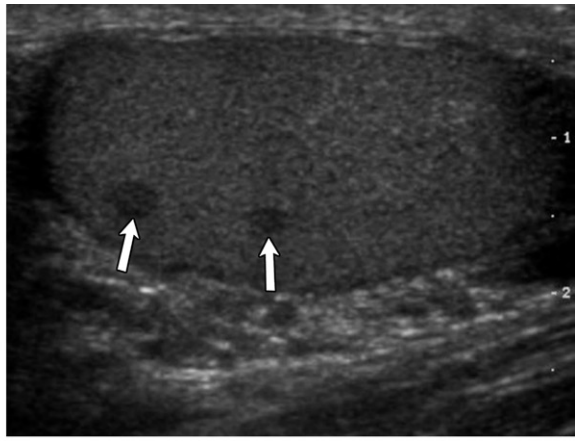

19.

Figures 18, 19. **(18)** Renal sarcoidosis in a 42-year-old man. Axial CT image of the abdomen shows many hypoattenuating lesions in the kidneys (arrowheads) bilaterally. Upper abdominal adenopathy (arrows) is also present. Conditions considered in the differential diagnosis included metastases, lymphoma, pyelonephritis, interstitial nephritis, and immunoglobulin G4–related renal disease. A diagnosis of sarcoidosis was confirmed on the basis of biopsy results. **(19)** Testicular sarcoidosis in a 33-year-old man. Longitudinal US image of the right testicle shows scattered hypoechoic lesions (arrows). Lesions with a similar appearance were also seen in the left testicle (not shown). The patient had a known diagnosis of sarcoidosis, and concurrent CT of the chest showed bilateral hilar adenopathy, consistent with multisystem sarcoid involvement.

kidney (2,89,90). Sarcoidosis causes abnormal calcium metabolism, which may result in hypercalcemia (in 10% of patients), hypercalciuria (in 30%–40% of patients), and renal calculi (in 10% of patients) (2,89,90). Sarcoid macrophages possess 25-hydroxyvitamin D–1α-hydroxylase, which converts 25-hydroxyvitamin D to the more active vitamin D metabolite calcitriol (1,25 dihydroxyvitamin D) (2,89,90). Normally, the production of calcitriol from 25-hydroxyvitamin D is regulated by parathyroid hormone, but in patients with sarcoidosis, the activated macrophages produce calcitriol independently, without the regulation of parathyroid hormone. This leads to excessive calcitriol-induced intestinal calcium absorption, with resultant hypercalcemia and hypercalciuria. Underlying renal function usually is maintained, but severe granulomatous nephritis or substantial intrarenal calcium deposition rarely may result in renal failure. The lesions are hypovascular on CT images, causing a range of enhancement patterns from mottled or striated to the less frequently seen mass-like areas. CT may show nephromegaly, atrophy, or multifocal bilateral hypointense hypovascular masses (Fig 18). However, other conditions such as lymphoma, metastases, hypovascular renal cell carcinoma, and infection also may produce a similar appearance and should be considered in the differential diagnosis.

Sarcoidosis also can affect the testes and epididymis. US may show multiple unilateral

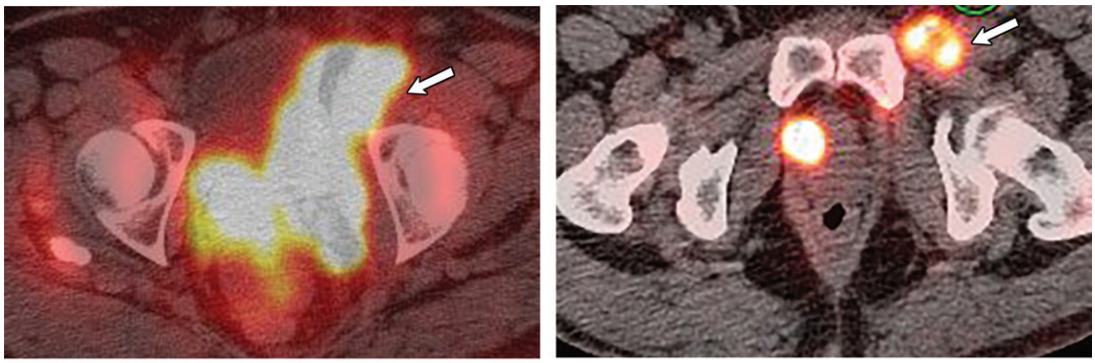

a. b.

Figure 20. Sarcoidosis in a 62-year-old woman. Axial fused PET/CT images of the pelvis show a markedly FDG-avid mass in the pelvis, which is confluent with bulky left external iliac adenopathy (arrow in **a**), and an FDG-avid inguinal node (arrow in **b**). A diagnosis of sarcoidosis was confirmed on the basis of biopsy results.

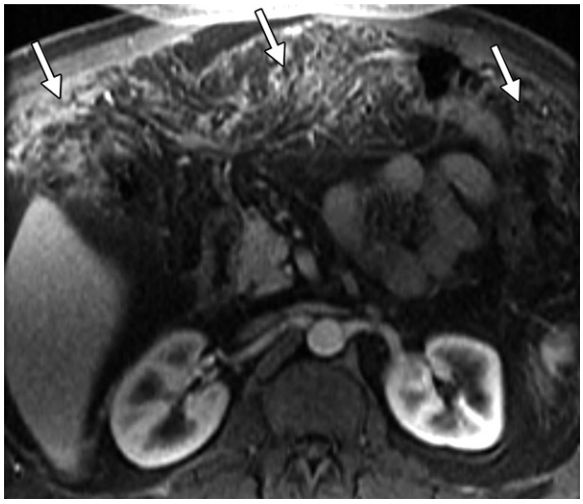

Figure 21. Peritoneal sarcoidosis in a 47-year-old man. Axial contrast-enhanced T1-weighted MR image shows nodular thickening and enhancement in the peritoneum (arrows). This appearance is nonspecific because peritoneal carcinomatosis, peritoneal lymphomatosis, and infectious conditions such as tuberculosis also may cause a similar appearance. A diagnosis of peritoneal sarcoidosis was confirmed on the basis of biopsy results.

or bilateral hypoechoic lesions in the testes and epididymis (Fig 19). Again, lymphoma, leukemia, metastases, and other granulomatous diseases are the main considerations in the differential diagnosis.

Abdominal and pelvic adenopathy may be seen in 30% of patients (83,85–87). Any nodal station may be involved, but upper abdominal nodes more commonly are involved compared with pelvic nodes. Usually, sarcoidosis-related adenopathy tends to be smaller than that in patients with lymphoma. Also, confluent nodal masses and involvement of retrocrural nodes are seen less frequently than they are in lymphoma. However, these findings are not specific, because massively enlarged nodes and retrocrural adenopathy have been known to develop in sarcoidosis (86). Sarcoidosis-related adenopathy also may be FDG avid, making it difficult to exclude other causes such as lymphoma or metastases (Fig 20).

The peritoneum is a rare site of involvement in sarcoidosis and may show nonspecific imaging findings such as ascites, diffuse peritoneal stranding, or discrete focal peritoneal nodules (Fig 21) (23). However, tissue diagnosis is often required to differentiate it from peritoneal carcinomatosis or atypical infections such as tuberculosis.

Musculoskeletal Sarcoidosis

Sarcoidosis can involve the bones, joints, and muscles. Osseous involvement in sarcoidosis occurs in 1%–13% of patients, with an estimated average occurrence of 5% (91). Although sarcoidosis can involve any bones in the axial and appendicular skeleton, small bones of the hand (in particular, the distal and middle phalanges of the second and third digits) are involved more commonly (23). Soft-tissue thickening may be seen surrounding the fingers and is referred to as "sausage dactylitis." At radiography, a lace-like pattern of osteolysis with thickened trabeculae and a thin cortex are characteristically seen in the small bones of the hands and feet (Fig 22). A periosteal reaction is typically absent. Pathologic fractures with bone collapse and misalignment may occur because of sarcoid osteolysis.

Sarcoid involvement of the long bones of the extremities and axial skeleton is relatively uncommon. Radiography and bone scintigraphy may not be sensitive for identifying sarcoid involvement at these sites (23,92). CT may reveal lytic lesions with or without peripheral sclerosis. MR imaging is more sensitive for identification of osseous abnormalities and the extent of marrow, soft-tissue, and tendon involvement (92). However, MR imaging is not specific and may show a

Figure 22. Osseous sarcoidosis in a 43-year-old man. Radiograph of the left hand shows lace-like osteolysis in the phalanges, with multiple well-defined lytic lesions (arrows). Note the preservation of joint space and the absence of periosteal reaction.

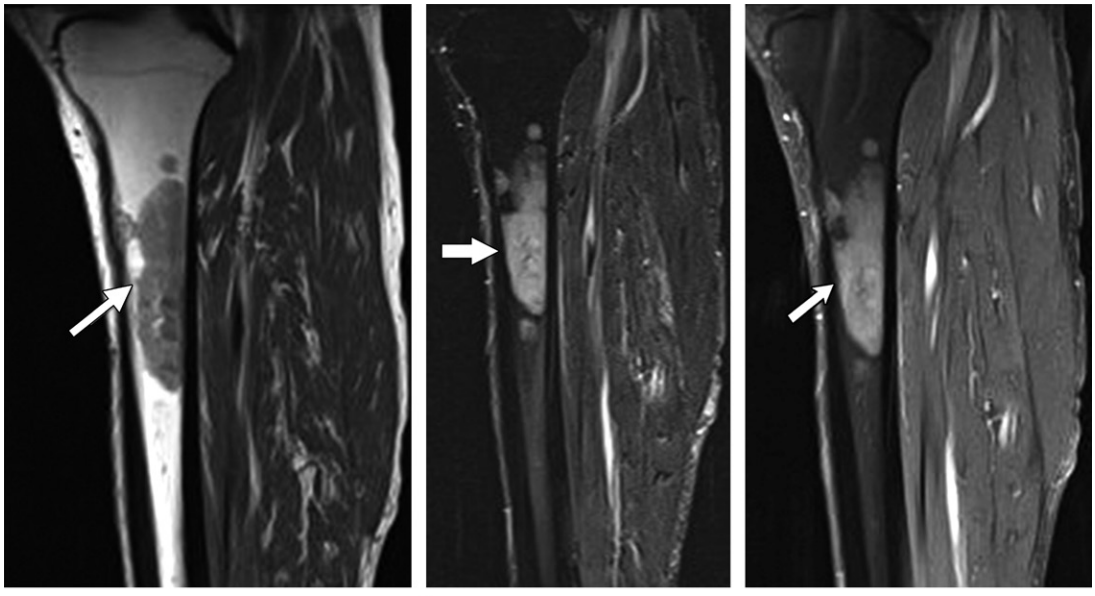

a. **b.** **c.**

Figure 23. Osseous sarcoidosis in a 57-year-old man. **(a)** Sagittal T1-weighted MR image shows a large hypointense intramedullary lesion in the left tibia (arrow). A smaller lesion is seen superior to this. **(b)** Sagittal short inversion-time inversion-recovery (STIR) MR image shows heterogeneous high signal intensity in the lesion (arrow). **(c)** Sagittal fat-suppressed contrast-enhanced T1-weighted MR image shows avid enhancement in the intramedullary lesions (arrow). A diagnosis of sarcoidosis was confirmed on the basis of biopsy results.

variable appearance including well-defined, focal T1-hypointense, T2-hyperintense, and enhancing intramedullary lesions or poorly defined infiltrative processes in the bone marrow (Figs 23, 24). The corroborative clinical history of sarcoidosis may be helpful, but often biopsy is required to differentiate these from metastases or marrow neoplastic disorders such as lymphoma.

Sarcoid involvement of the joints is relatively common and is classified as acute arthritis or chronic or recurrent arthritis (93,94). Sarcoid arthritis tends to be more common in young women (<40 years old). The acute phase may manifest in 10%–40% of cases. Usually, it is seen early in the course of the disease (within 6 months of diagnosis) and is typically self limiting (93,94). Löfgren syndrome refers to acute sarcoidosis characterized by the combination of erythema nodosum, bilateral hilar adenopathy, polyarthritis, and constitutional symptoms (3,6,13,18). Polyarthritis or oligoarthritis is much more common than is monoarthritis. The ankles, knees, wrists, proximal interphalangeal joints, metacarpophalangeal joints, and elbows are the

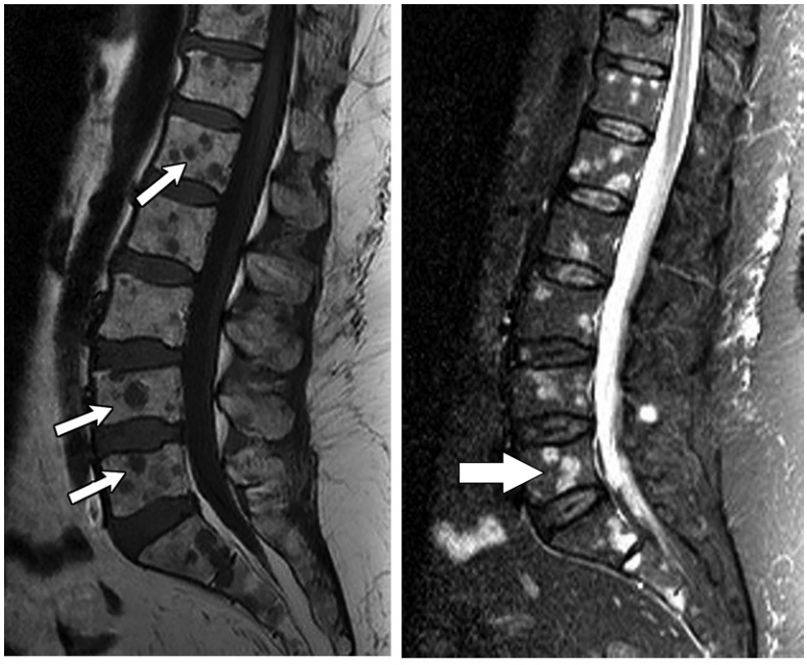

a. b.

Figure 24. Sarcoidosis in a 62-year-old woman. **(a)** Sagittal T1-weighted MR image of the lumbar spine shows numerous T1-hypointense lesions (arrows) in the lumbar vertebrae. **(b)** Sagittal short inversion time inversion-recovery (STIR) MR image of the lumbar spine demonstrates T2-hyperintense lesions (arrow) in the lumbar spine. Biopsy of the bone lesion confirmed sarcoidosis.

commonly affected sites. Presenting symptoms include swelling, pain, erythema, tenderness, and reduced mobility and range of motion.

When the symptoms of sarcoid arthritis have persisted more than 6 months after the diagnosis of sarcoidosis, it is considered chronic sarcoid arthritis. In comparison with acute arthritis, the chronic form is seen infrequently, manifesting in 1%–4% of patients. Patients may develop oligoarthritis involving the ankles or knees. Symptoms may recede, but recurrence is not uncommon. MR imaging may show the full extent of arthritis and reveal concurrent abnormalities such as tenosynovitis, tendonitis, bursitis, and synovitis (23,92).

Asymptomatic muscular involvement may develop in 25%–80% of patients with sarcoidosis. However, symptomatic involvement is rare, manifesting in less than 0.5% of patients (6,93). When it is symptomatic, patients may present with features of acute myositis (fever, myalgia, muscle weakness), nodular sarcoidosis (palpable nodules that may be painful or tender), or chronic myopathy (proximal muscle weakness, muscle atrophy, muscle contractures). Involvement of the respiratory skeletal muscles may result in dyspnea. Nodular sarcoid myopathy can manifest as single or multifocal soft-tissue masses, often involving the lower extremities. In nodular sarcoid myopathy, lesions may have a star-shaped area of low signal intensity in the center and high signal intensity in the periphery on T2-weighted images (ie, the "dark star" appearance) (95).

MR imaging can show the degree of granulomatous infiltration and the extent of fatty atrophy and also may help to guide biopsy, because the differential diagnosis includes polymyositis and steroid-induced myopathy (92). Subcutaneous involvement in sarcoidosis may manifest as focal or diffuse infiltrative lesions. These may be hypoechoic at US, while CT may show soft-tissue-attenuation nodules. On MR images, lesions tend to be T1 hypointense compared with muscle and T2 hyperintense, with mild enhancement on postcontrast images (92).

Cutaneous Sarcoidosis

There is a spectrum of cutaneous manifestations in sarcoidosis that may develop in 20%–35% of patients (2,3,13,96). The lesions specific for sarcoidosis include maculopapule, nodule, plaque, subcutaneous nodule, infiltrative scar, and lupus pernio (2,3,13,96). Erythema nodosum; calcifications; prurigo; erythema multiforme; and nail changes such as clubbing, onycholysis, and subungual hyperkeratosis are the nonspecific findings seen in sarcoidosis (2,3,13,96). Papules are the most common manifestations and are typically tiny flesh-colored, red, or yellow lesions seen around the eyes and nasolabial folds and in

the head and neck regions (96). Lupus pernio, the most characteristic specific cutaneous manifestation of sarcoidosis, appears as reddish-purple plaques associated with prominent telangiectasia and typically are seen in the nose, ear, cheek, and hand (96).

Erythema nodosum, the other well-known but nonspecific cutaneous lesion in sarcoidosis, is thought to represent a hypersensitivity reaction to a hitherto unknown antigen (96). The lesions manifest as tender erythematous subcutaneous nodules on the shin and are usually associated with acute sarcoidosis. Löfgren syndrome refers to the constellation of erythema nodosum, bilateral hilar adenopathy, arthralgia, and fever and is thought to be virtually diagnostic for sarcoidosis, obviating the need for histopathologic confirmation (2,52,79).

Sarcoid-like Reactions

Sarcoid reactions or sarcoid-like reactions refer to the manifestation of noncaseating granulomas in patients with known malignancies, which can develop in the regional lymph nodes that drain a tumor site, in the tumor itself, or at other sites, without the systemic manifestations of sarcoidosis (Figs 25, 26) (97). Sarcoid reactions can develop during chemotherapy or immunotherapy and may cause substantial confusion, because they could be misconstrued to be progressive or recurrent disease. Similar to malignancies, sarcoid-like reactions also can demonstrate uptake of FDG at PET/CT, which can make it extremely difficult to differentiate between these two entities (98). Chowdhury et al (98) reviewed FDG PET/CT studies in 23 patients with sarcoid-like reactions and reported that 100% of them had mediastinal nodal FDG uptake, 85% had symmetrical hilar uptake, and 65% had extrathoracic uptake, including that in the abdominal nodes, liver, and spleen (Figs 25, 26) .We suggest that awareness of the pattern of FDG uptake in sarcoid reactions may help to avoid misinterpretation of these as progressive disease, but tissue diagnosis may be necessary in most cases for definitive confirmation (98).

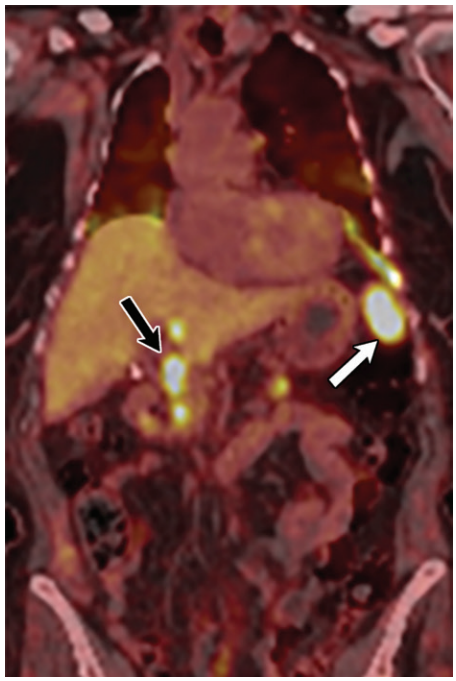

Figure 25. Sarcoid-like reaction in a 68-year-old man with lymphoma. Coronal fused PET/CT image shows avid FDG uptake in the spleen (white arrow) and upper abdominal nodes (black arrow). CT-guided biopsy of the abdominal node was performed. Results of pathologic analysis showed the presence of noncaseating granuloma and were negative for tumor cells.

Management

Currently available treatment options are not curative, but rather are aimed at controlling the granulomatous process. Given the high probability of spontaneous resolution in patients with newly diagnosed early-stage pulmonary sarcoidosis, it may be preferable to monitor patients, without specific treatment in the early stages (2,3). Patients showing progression of symptoms, a worsening radiographic appearance, or decreasing pulmonary function should be considered for treatment (3). Indications for systemic treatment also include extrapulmonary diseases such as cardiac, central nervous system, renal, ocular, and cutaneous sarcoidosis (those that do not respond to topical therapy) and symptomatic hypercalcemia (2,3,13). Systemic corticosteroids are the mainstay of treatment in sarcoidosis (2,3). Patients who experience disease progression while taking steroids or those in whom steroids are contraindicated may be considered for other medications such as antimalarial drugs, tetracycline, methotrexate, azathioprine, leflunomide, cyclophosphamide, mycophenolate mofetil, pentoxifylline, infliximab, rituximab, and adalimumab (3,20). Patients should be monitored closely for adverse effects, given the high toxicity of these treatment regimens. Patients with advanced-stage disease involving the lungs, liver, heart, or kidneys may be considered for organ transplantation.

Although no strict guidelines currently are available for follow-up, the suggestion is that patients undergo clinical examination and chest radiography every 3–6 months. It also is reasonable to monitor patients with pulmonary function tests, electrocardiography, and checking of serum creatinine and calcium levels every 6 months (3). Patients who demonstrate response to steroid therapy should be monitored and

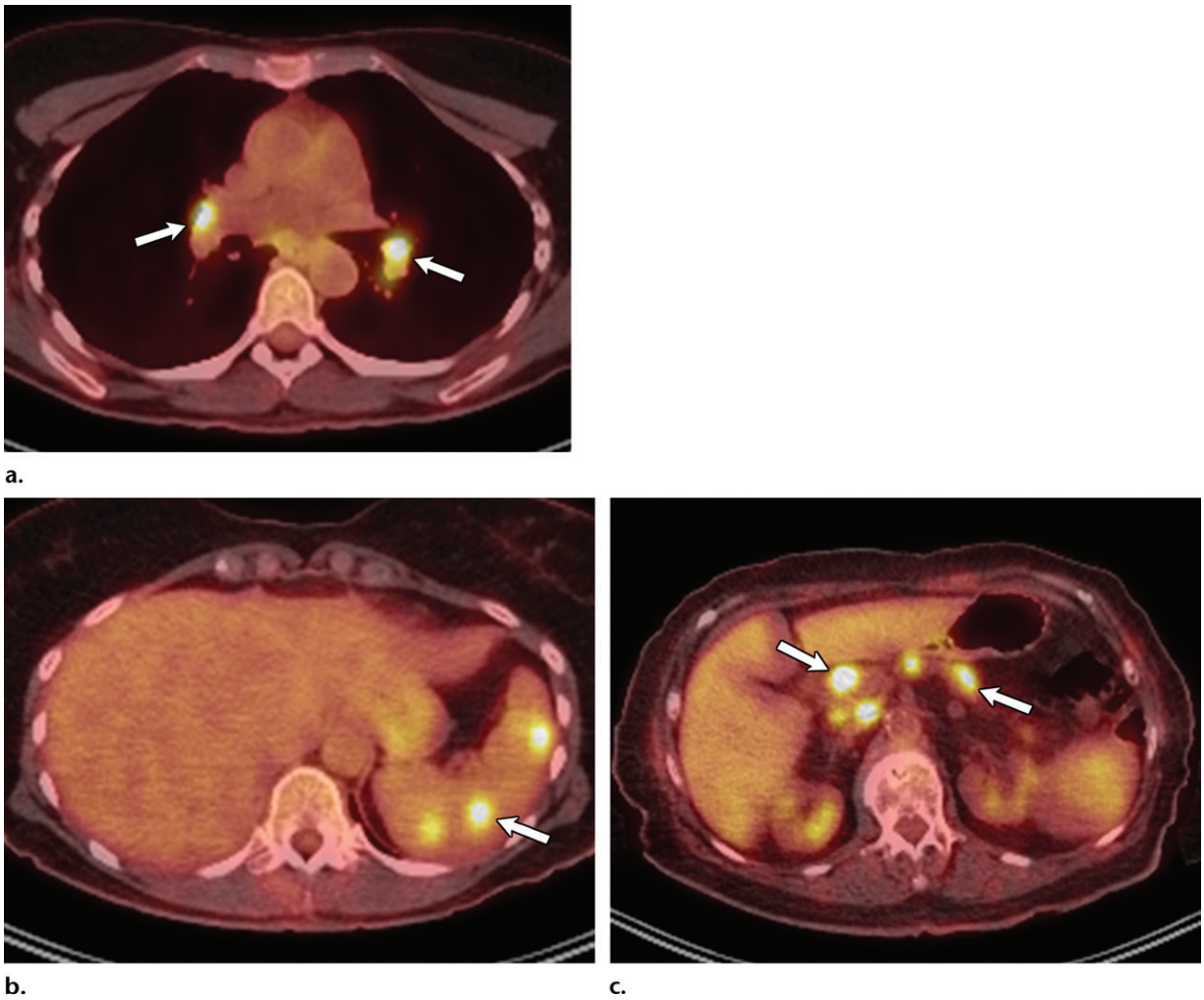

Figure 26. Sarcoid-like reaction in a 38-year-old woman with melanoma who was undergoing immunotherapy. Axial fused PET/CT images show FDG-avid bilateral hilar adenopathy (arrows in **a**), numerous focal splenic lesions (arrow in **b**), and upper abdominal nodes (arrows in **c**). Although this pattern of symmetrical hilar adenopathy with splenic and upper abdominal nodal involvement is suggestive of a sarcoid-like reaction, the differential diagnosis would include evaluation for recurrent disease. The results of pathologic analysis showed the presence of noncaseating granuloma and were negative for tumor cells.

followed up for at least 3 years because approximately 37%–74% of treated patients show relapse within that time period (3).

Approximately 25%–30% of patients may develop chronic sarcoidosis (disease duration ≥3 years). Substantial morbidity can ensue in these patients and includes pulmonary fibrosis, pulmonary hypertension, aspergilloma, and cardiac failure (3,99). Pulmonary failure is the most important cause of death in patients with sarcoidosis in the United States, while cardiac sarcoidosis is the most common cause for sarcoidosis-related death in Japan (3,99). Indeed, advanced-stage sarcoidosis confers a significantly higher mortality rate (0.5%–5%) than that in the general population (20,99).

Conclusion

Sarcoidosis can affect multiple organ systems in the body. Clinical manifestations usually are nonspecific, which can lead to delayed diagnosis. Although early-stage sarcoidosis may be associated with an excellent prognosis, advanced-stage disease can cause substantial morbidity and mortality. Radiologists should be aware of the imaging features of both pulmonary and extrapulmonary sarcoidosis. Radiologists play an important role in the management of sarcoidosis. Frequently, a radiologist may be the first person to suggest this diagnosis on the basis of imaging features, even when the diagnosis is not clinically suspected. Furthermore, in patients with characteristic clinical features suggestive of sarcoidosis such as Löfgren's syndrome, the presence of classic imaging findings may help to confirm the diagnosis. Finally, imaging is increasingly being used for monitoring therapeutic response and identifying complications related to sarcoidosis. Therefore, familiarity with the imaging features of sarcoidosis may help in diagnosing, evaluating the extent of disease, and guiding optimal patient care.

Acknowledgment.—We would like to thank Kelly Kage, MFA, for preparing the images.

Disclosures of Conflicts of Interest.—**M.G.L.** *Activities related to the present article:* disclosed no relevant relationships. *Activities not related to the present article:* grants pending from Ethicon and Philips. *Other activities:* disclosed no relevant relationships. **P.J.P.** *Activities related to the present article:* disclosed no relevant relationships. *Activities not related to the present article:* consultancy for Bracco and Check Cap, royalties from Elsevier, and stock/stock options from Cellactar, Elucent, Shine, and VirtuoCTC. *Other activities:* disclosed no relevant relationships. **K.S.** *Activities related to the present article:* disclosed no relevant relationships. *Activities not related to the present article:* consultant for Guerbet. *Other activities:* disclosed no relevant relationships.

References

1. Rybicki BA, Major M, Popovich J Jr, Maliarik MJ, Iannuzzi MC. Racial differences in sarcoidosis incidence: a 5-year study in a health maintenance organization. Am J Epidemiol 1997;145(3):234–241
2. Iannuzzi MC, Rybicki BA, Teirstein AS. Sarcoidosis. N Engl J Med 2007;357(21):2153–2165.
3. Valeyre D, Prasse A, Nunes H, Uzunhan Y, Brillet PY, Müller-Quernheim J. Sarcoidosis. Lancet 2014;383(9923):1155–1167.
4. Hillerdal G, Nöu E, Osterman K, Schmekel B. Sarcoidosis: epidemiology and prognosis—a 15-year European study. Am Rev Respir Dis 1984;130(1):29–32.
5. Rybicki BA, Iannuzzi MC, Frederick MM, et al. Familial aggregation of sarcoidosis: a case-control etiologic study of sarcoidosis (ACCESS). Am J Respir Crit Care Med 2001;164(11):2085–2091.
6. Baughman RP, Teirstein AS, Judson MA, et al. Clinical characteristics of patients in a case control study of sarcoidosis. Am J Respir Crit Care Med 2001;164(10 Pt 1):1885–1889.
7. Girvin F, Zeig-Owens R, Gupta D, et al. Radiologic features of World Trade Center-related sarcoidosis in exposed NYC Fire Department rescue workers. J Thorac Imaging 2016;31(5):296–303.
8. Esteves T, Aparicio G, Garcia-Patos V. Is there any association between sarcoidosis and infectious agents? a systematic review and meta-analysis. BMC Pulm Med 2016;16(1):165.
9. McGrath DS, Daniil Z, Foley P, et al. Epidemiology of familial sarcoidosis in the UK. Thorax 2000;55(9):751–754.
10. Sverrild A, Backer V, Kyvik KO, et al. Heredity in sarcoidosis: a registry-based twin study. Thorax 2008;63(10):894–896.
11. Sato H, Grutters JC, Pantelidis P, et al. HLA-DQB1*0201: a marker for good prognosis in British and Dutch patients with sarcoidosis. Am J Respir Cell Mol Biol 2002;27(4):406–412.
12. Rybicki BA, Sinha R, Iyengar S, et al. Genetic linkage analysis of sarcoidosis phenotypes: the sarcoidosis genetic analysis (SAGA) study. Genes Immun 2007;8(5):379–386.
13. Iannuzzi MC, Fontana JR. Sarcoidosis: clinical presentation, immunopathogenesis, and therapeutics. JAMA 2011;305(4):391–399.
14. Loke WS, Herbert C, Thomas PS. Sarcoidosis: immunopathogenesis and immunological markers. Int J Chronic Dis 2013;2013:928601.
15. Gal AA, Koss MN. The pathology of sarcoidosis. Curr Opin Pulm Med 2002;8(5):445–451.
16. Ma Y, Gal A, Koss MN. The pathology of pulmonary sarcoidosis: update. Semin Diagn Pathol 2007;24(3):150–161.
17. Statement on sarcoidosis: Joint Statement of the American Thoracic Society (ATS), the European Respiratory Society (ERS) and the World Association of Sarcoidosis and Other Granulomatous Disorders (WASOG) adopted by the ATS Board of Directors and by the ERS Executive Committee, February 1999. Am J Respir Crit Care Med 1999;160(2):736–755.
18. Baughman RP, Culver DA, Judson MA. A concise review of pulmonary sarcoidosis. Am J Respir Crit Care Med 2011;183(5):573–581.
19. Lynch JP 3rd, Ma YL, Koss MN, White ES. Pulmonary sarcoidosis. Semin Respir Crit Care Med 2007;28(1):53–74.
20. Nunes H, Brillet PY, Valeyre D, Brauner MW, Wells AU. Imaging in sarcoidosis. Semin Respir Crit Care Med 2007;28(1):102–120.
21. Criado E, Sánchez M, Ramírez J, et al. Pulmonary sarcoidosis: typical and atypical manifestations at high-resolution CT with pathologic correlation. RadioGraphics 2010;30(6):1567–1586.
22. Scadding JG. Prognosis of intrathoracic sarcoidosis in England: a review of 136 cases after five years' observation. BMJ 1961;2(5261):1165–1172.
23. Koyama T, Ueda H, Togashi K, Umeoka S, Kataoka M, Nagai S. Radiologic manifestations of sarcoidosis in various organs. RadioGraphics 2004;24(1):87–104.
24. Van den Heuvel DA, de Jong PA, Zanen P, et al. Chest computed tomography-based scoring of thoracic sarcoidosis: inter-rater reliability of CT abnormalities. Eur Radiol 2015;25(9):2558–2566.
25. Walsh SL, Wells AU, Sverzellati N, et al. An integrated clinicoradiological staging system for pulmonary sarcoidosis: a case-cohort study. Lancet Respir Med 2014;2(2):123–130.
26. Guidry C, Fricke RG, Ram R, Pandey T, Jambhekar K. Imaging of sarcoidosis: a contemporary review. Radiol Clin North Am 2016;54(3):519–534.
27. Hawtin KE, Roddie ME, Mauri FA, Copley SJ. Pulmonary sarcoidosis: the 'great pretender.' Clin Radiol 2010;65(8):642–650.
28. Nishino M, Lee KS, Itoh H, Hatabu H. The spectrum of pulmonary sarcoidosis: variations of high-resolution CT findings and clues for specific diagnosis. Eur J Radiol 2010;73(1):66–73.
29. Abehsera M, Valeyre D, Grenier P, Jaillet H, Battesti JP, Brauner MW. Sarcoidosis with pulmonary fibrosis: CT patterns and correlation with pulmonary function. AJR Am J Roentgenol 2000;174(6):1751–1757.
30. Handa T, Nagai S, Miki S, et al. Incidence of pulmonary hypertension and its clinical relevance in patients with sarcoidosis. Chest 2006;129(5):1246–1252.
31. Pena TA, Soubani AO, Samavati L. Aspergillus lung disease in patients with sarcoidosis: a case series and review of the literature. Lung 2011;189(2):167–172.
32. Promteangtrong C, Salavati A, Cheng G, Torigian DA, Alavi A. The role of positron emission tomography-computed tomography/magnetic resonance imaging in the management of sarcoidosis patients. Hell J Nucl Med 2014;17(2):123–135.
33. Treglia G, Annunziata S, Sobic-Saranovic D, Bertagna F, Caldarella C, Giovanella L. The role of 18F-FDG-PET and PET/CT in patients with sarcoidosis: an updated evidence-based review. Acad Radiol 2014;21(5):675–684.
34. Keijsers RG, Grutters JC, Thomeer M, et al. Imaging the inflammatory activity of sarcoidosis: sensitivity and inter observer agreement of (67)Ga imaging and (18)F-FDG PET. Q J Nucl Med Mol Imaging 2011;55(1):66–71.
35. Braun JJ, Kessler R, Constantinesco A, Imperiale A. 18F-FDG PET/CT in sarcoidosis management: review and report of 20 cases. Eur J Nucl Med Mol Imaging 2008;35(8):1537–1543.
36. Mostard RL, Verschakelen JA, van Kroonenburgh MJ, et al. Severity of pulmonary involvement and (18)F-FDG PET activity in sarcoidosis. Respir Med 2013;107(3):439–447.
37. Mostard RL, Prompers L, Weijers RE, et al. F-18 FDG PET/CT for detecting bone and bone marrow involvement in sarcoidosis patients. Clin Nucl Med 2012;37(1):21–25.
38. Mostard RL, Vöö S, van Kroonenburgh MJ, et al. Inflammatory activity assessment by F18 FDG-PET/CT in persistent symptomatic sarcoidosis. Respir Med 2011;105(12):1917–1924.
39. Leverve XM, Fontaine E, Putod-Paramelle F, Rigoulet M. Decrease in cytosolic ATP/ADP ratio and activation of pyruvate kinase after in vitro addition of almitrine in hepatocytes isolated from fasted rats. Eur J Biochem 1994;224(3):967–974.
40. Keijsers RG, Verzijlbergen EJ, van den Bosch JM, et al. 18F-FDG PET as a predictor of pulmonary function in sarcoidosis. Sarcoidosis Vasc Diffuse Lung Dis 2011;28(2):123–129.
41. Keijsers RG, Verzijlbergen JF, van Diepen DM, van den Bosch JM, Grutters JC. 18F-FDG PET in sarcoidosis: an observational study in 12 patients treated with infliximab. Sarcoidosis Vasc Diffuse Lung Dis 2008;25(2):143–149.
42. Milman N, Graudal N, Loft A, Mortensen J, Larsen J, Baslund B. Effect of the TNF-α inhibitor adalimumab in patients with

recalcitrant sarcoidosis: a prospective observational study using FDG-PET. Clin Respir J 2012;6(4):238–247.
43. Sobic-Saranovic DP, Grozdic IT, Videnovic-Ivanov J, et al. Responsiveness of FDG PET/CT to treatment of patients with active chronic sarcoidosis. Clin Nucl Med 2013;38(7):516–521.
44. Silverman KJ, Hutchins GM, Bulkley BH. Cardiac sarcoid: a clinicopathologic study of 84 unselected patients with systemic sarcoidosis. Circulation 1978;58(6):1204–1211.
45. Birnie DH, Nery PB, Ha AC, Beanlands RS. Cardiac sarcoidosis. J Am Coll Cardiol 2016;68(4):411–421.
46. Nagai T, Kohsaka S, Okuda S, Anzai T, Asano K, Fukuda K. Incidence and prognostic significance of myocardial late gadolinium enhancement in patients with sarcoidosis without cardiac manifestation. Chest 2014;146(4):1064–1072.
47. Mehta D, Lubitz SA, Frankel Z, et al. Cardiac involvement in patients with sarcoidosis: diagnostic and prognostic value of outpatient testing. Chest 2008;133(6):1426–1435.
48. Ipek E, Demirelli S, Ermis E, Inci S. Sarcoidosis and the heart: a review of the literature. Intractable Rare Dis Res 2015;4(4):170–180.
49. Kim JS, Judson MA, Donnino R, et al. Cardiac sarcoidosis. Am Heart J 2009;157(1):9–21.
50. Nery PB, Mc Ardle BA, Redpath CJ, et al. Prevalence of cardiac sarcoidosis in patients presenting with monomorphic ventricular tachycardia. Pacing Clin Electrophysiol 2014;37(3):364–374.
51. Birnie DH, Sauer WH, Bogun F, et al. HRS expert consensus statement on the diagnosis and management of arrhythmias associated with cardiac sarcoidosis. Heart Rhythm 2014;11(7):1305–1323.
52. Diagnostic standard and guidelines for sarcoidosis [in Japanese]. Jpn J Sarcoidosis Granulomatous Disord 2007;27:89–102.
53. Ichinose A, Otani H, Oikawa M, et al. MRI of cardiac sarcoidosis: basal and subepicardial localization of myocardial lesions and their effect on left ventricular function. AJR Am J Roentgenol 2008;191(3):862–869.
54. Cummings KW, Bhalla S, Javidan-Nejad C, Bierhals AJ, Gutierrez FR, Woodard PK. A pattern-based approach to assessment of delayed enhancement in nonischemic cardiomyopathy at MR imaging. RadioGraphics 2009;29(1):89–103.
55. Vogel-Claussen J, Rochitte CE, Wu KC, et al. Delayed enhancement MR imaging: utility in myocardial assessment. RadioGraphics 2006;26(3):795–810.
56. Mc Ardle BA, Leung E, Ohira H, et al. The role of F(18)-fluorodeoxyglucose positron emission tomography in guiding diagnosis and management in patients with known or suspected cardiac sarcoidosis. J Nucl Cardiol 2013;20(2):297–306.
57. Blankstein R, Osborne M, Naya M, et al. Cardiac positron emission tomography enhances prognostic assessments of patients with suspected cardiac sarcoidosis. J Am Coll Cardiol 2014;63(4):329–336.
58. Jeudy J, Burke AP, White CS, Kramer GB, Frazier AA. Cardiac sarcoidosis: the challenge of radiologic-pathologic correlation. RadioGraphics 2015;35(3):657–679.
59. Youssef G, Leung E, Mylonas I, et al. The use of 18F-FDG PET in the diagnosis of cardiac sarcoidosis: a systematic review and metaanalysis including the Ontario experience. J Nucl Med 2012;53(2):241–248.
60. Tang R, Wang JT, Wang L, et al. Impact of patient preparation on the diagnostic performance of 18F-FDG PET in cardiac sarcoidosis: a systematic review and meta-analysis. Clin Nucl Med 2016;41(7):e327–e339.
61. Ohira H, Tsujino I, Ishimaru S, et al. Myocardial imaging with 18F-fluoro-2-deoxyglucose positron emission tomography and magnetic resonance imaging in sarcoidosis. Eur J Nucl Med Mol Imaging 2008;35(5):933–941.
62. Chareonthaitawee P, Beanlands RS, Chen W, et al. Joint SNMMI-ASNC expert consensus document on the role of (18)F-FDG PET/CT in cardiac sarcoid detection and therapy monitoring. J Nucl Cardiol 2017;24(5):1741–1758.
63. Osborne MT, Hulten EA, Singh A, et al. Reduction in ^{18}F-fluorodeoxyglucose uptake on serial cardiac positron emission tomography is associated with improved left ventricular ejection fraction in patients with cardiac sarcoidosis. J Nucl Cardiol 2014;21(1):166–174.
64. Matthews R, Bench T, Meng H, Franceschi D, Relan N, Brown DL. Diagnosis and monitoring of cardiac sarcoidosis with delayed-enhanced MRI and 18F-FDG PET-CT. J Nucl Cardiol 2012;19(4):807–810.
65. Keijsers RG, Verzijlbergen FJ, Rensing BJ, Grutters JC. Cardiac sarcoidosis: a challenge to measure disease activity. J Nucl Cardiol 2008;15(4):595–598.
66. Casset-Senon D, Philippe L, Renard JP, Cosnay P. Recurrent ventricular tachycardia in cardiac sarcoidosis: usefulness of fluorodeoxyglucose positron emission tomography for adequate management of corticoid therapy after placement of an implantable cardioverter defibrillator. J Nucl Cardiol 2008;15(2):282–285.
67. Takeda N, Yokoyama I, Hiroi Y, et al. Positron emission tomography predicted recovery of complete A-V nodal dysfunction in a patient with cardiac sarcoidosis. Circulation 2002;105(9):1144–1145.
68. Iwai K, Tachibana T, Takemura T, Matsui Y, Kitaichi M, Kawabata Y. Pathological studies on sarcoidosis autopsy. I. Epidemiological features of 320 cases in Japan. Acta Pathol Jpn 1993;43(7-8):372–376.
69. Zajicek JP, Scolding NJ, Foster O, et al. Central nervous system sarcoidosis: diagnosis and management. QJM 1999;92(2):103–117.
70. Shah R, Roberson GH, Curé JK. Correlation of MR imaging findings and clinical manifestations in neurosarcoidosis. AJNR Am J Neuroradiol 2009;30(5):953–961.
71. Lexa FJ, Grossman RI. MR of sarcoidosis in the head and spine: spectrum of manifestations and radiographic response to steroid therapy. AJNR Am J Neuroradiol 1994;15(5):973–982.
72. Smith JK, Matheus MG, Castillo M. Imaging manifestations of neurosarcoidosis. AJR Am J Roentgenol 2004;182(2):289–295.
73. Dumas JL, Valeyre D, Chapelon-Abric C, et al. Central nervous system sarcoidosis: follow-up at MR imaging during steroid therapy. Radiology 2000;214(2):411–420.
74. Huang JF, Aksamit AJ, Staff NP. MRI and PET imaging discordance in neurosarcoidosis. Neurology 2012;79(10):1070.
75. Sakushima K, Yabe I, Shiga T, et al. FDG-PET SUV can distinguish between spinal sarcoidosis and myelopathy with canal stenosis. J Neurol 2011;258(2):227–230.
76. Aide N, Benayoun M, Kerrou K, Khalil A, Cadranel J, Talbot JN. Impact of [18F]-fluorodeoxyglucose ([18F]-FDG) imaging in sarcoidosis: unsuspected neurosarcoidosis discovered by [18F]-FDG PET and early metabolic response to corticosteroid therapy. Br J Radiol 2007;80(951):e67–e71.
77. Dash GI, Kimmelman CP. Head and neck manifestations of sarcoidosis. Laryngoscope 1988;98(1):50–53.
78. Badhey AK, Kadakia S, Carrau RL, Iacob C, Khorsandi A. Sarcoidosis of the head and neck. Head Neck Pathol 2015;9(2):260–268.
79. Lynch JP 3rd, Sharma OP, Baughman RP. Extrapulmonary sarcoidosis. Semin Respir Infect 1998;13(3):229–254.
80. Bodaghi B, Touitou V, Fardeau C, Chapelon C, LeHoang P. Ocular sarcoidosis. Presse Med 2012;41(6 Pt 2):e349–e354.
81. Chapman MN, Fujita A, Sung EK, et al. Sarcoidosis in the head and neck: an illustrative review of clinical presentations and imaging findings. AJR Am J Roentgenol 2017;208(1):66–75.
82. Kennedy PT, Zakaria N, Modawi SB, et al. Natural history of hepatic sarcoidosis and its response to treatment. Eur J Gastroenterol Hepatol 2006;18(7):721–726.
83. Warshauer DM, Lee JK. Imaging manifestations of abdominal sarcoidosis. AJR Am J Roentgenol 2004;182(1):15–28.
84. Kessler A, Mitchell DG, Israel HL, Goldberg BB. Hepatic and splenic sarcoidosis: ultrasound and MR imaging. Abdom Imaging 1993;18(2):159–163.
85. Folz SJ, Johnson CD, Swensen SJ. Abdominal manifestations of sarcoidosis in CT studies. J Comput Assist Tomogr 1995;19(4):573–579.
86. Warshauer DM, Dumbleton SA, Molina PL, Yankaskas BC, Parker LA, Woosley JT. Abdominal CT findings in sarcoidosis: radiologic and clinical correlation. Radiology 1994;192(1):93–98.
87. Britt AR, Francis IR, Glazer GM, Ellis JH. Sarcoidosis: abdominal manifestations at CT. Radiology 1991;178(1):91–94.

88. Karaosmanoğlu AD, Onur MR, Saini S, Taberi A, Karcaaltincaba M. Imaging of hepatobiliary involvement in sarcoidosis. Abdom Imaging 2015;40(8):3330–3337.
89. Mahévas M, Lescure FX, Boffa JJ, et al. Renal sarcoidosis: clinical, laboratory, and histologic presentation and outcome in 47 patients. Medicine (Baltimore) 2009;88(2):98–106.
90. Sharma OP. Vitamin D, calcium, and sarcoidosis. Chest 1996;109(2):535–539.
91. James DG, Neville E, Carstairs LS. Bone and joint sarcoidosis. Semin Arthritis Rheum 1976;6(1):53–81.
92. Moore SL, Teirstein AE. Musculoskeletal sarcoidosis: spectrum of appearances at MR imaging. RadioGraphics 2003;23(6):1389–1399.
93. Anakwenze OA, Kancherla V, Hatch M, Brooks JS, Ogilvie CM. Primary musculoskeletal sarcoidosis. Orthopedics 2010;33(5).
94. Zisman DA, Shorr AF, Lynch JP 3rd. Sarcoidosis involving the musculoskeletal system. Semin Respir Crit Care Med 2002;23(6):555–570.
95. Otake S, Banno T, Ohba S, Noda M, Yamamoto M. Muscular sarcoidosis: findings at MR imaging. Radiology 1990;176(1):145–148.
96. Sehgal VN, Riyaz N, Chatterjee K, Venkatash P, Sharma S. Sarcoidosis as a systemic disease. Clin Dermatol 2014;32(3):351–363.
97. Brincker H. Sarcoid reactions in malignant tumours. Cancer Treat Rev 1986;13(3):147–156.
98. Chowdhury FU, Sheerin F, Bradley KM, Gleeson FV. Sarcoid-like reaction to malignancy on whole-body integrated (18)F-FDG PET/CT: prevalence and disease pattern. Clin Radiol 2009;64(7):675–681.
99. Nardi A, Brillet PY, Letoumelin P, et al. Stage IV sarcoidosis: comparison of survival with the general population and causes of death. Eur Respir J 2011;38(6):1368–1373.